Research Article Vol. 38, No. 8 / August 2021 / Journal of the Optical Society of America B 2419

Journal of the Optical Society of America B

OPTICAL PHYSICS

Ability of gas modulation to reduce the pickup of drifts in refractometry

Ove Axner,[1,*] Clayton Forssén,[1] Isak Silander,[1] Johan Zakrisson,[1] and Martin Zelan[2]

[1]Department of Physics, Umeå University, SE-901 87 Umeå, Sweden
[2]Measurement Science and Technology, RISE Research Institutes of Sweden, SE-501 15 Borås, Sweden
*Corresponding author: ove.axner@umu.se

Received 27 January 2021; revised 2 July 2021; accepted 2 July 2021; posted 2 July 2021 (Doc. ID 420982); published 30 July 2021

Gas modulation refractometry (GAMOR) is a methodology for assessment of gas refractivity, molar density, and pressure that, by a rapid gas modulation, exhibits a reduced susceptibility to various types of disturbances. Although previously demonstrated experimentally, no detailed analysis of its ability to reduce the pickup of drifts has yet been given. This work provides an explication of to what extent modulated refractometry in general, and GAMOR in particular, can reduce drifts, predominantly those of the cavity lengths, gas leakages, and outgassing. It is indicated that the methodology is insensitive to the linear parts of so-called campaign-persistent drifts and that it has a significantly reduced susceptibility to others. This makes the methodology suitable for high-accuracy assessments and out-of-laboratory applications.

https://doi.org/10.1364/JOSAB.420982

1. INTRODUCTION

Fabry–Perot cavity (FPC)-based refractometry is a sensitive laser-based methodology for assessment of gas refractivity, molar density, and pressure. By measuring the refractivity, $n-1$, where n is the index of refraction, the density of the gas can be calculated by the use of the Lorentz–Lorenz equation, and, if its temperature is also measured, its pressure can be assessed by an equation of state [1]. The technique has demonstrated detection of gases with both high precision and good accuracy over a wide range of molar densities and pressures (for the latter, ranging from low millipascals to hundreds of kilopascals) [1–16]. Recent works have indicated that the methodology also has the potential to replace current pressure standards, in particular in the 1 Pa to 100 kPa range [17].

The methodology is built on the fact that the index of refraction constitutes the ratio of an optical length in the presence and absence of gas; for FPC-based refractometry, with and without gas in the cavity, here referred to as L $(=nL_0)$ and L_0, respectively. In practice, the optical lengths are assessed by measuring the frequency of a laser that is locked to a longitudinal mode of the cavity. By this, the shift of the frequency of the mode that takes place when gas is let into an FPC will be transferred to a shift in the frequency of the laser light [18]. Since frequency is the entity that can be assessed with highest accuracy in our society (up to one part in 10^{16} and potentially even one part in 10^{18}) [19], it opens up extraordinary abilities regarding precision and dynamic range. Hence, refractometry is therefore often based on FPCs [1,2,4,5,10,20,21].

The conventional means of assessing refractivity by the use of FPC-based refractometry is to assess L_0 and L in two separate assessments. However, in practice, this is not trivial, since experimental systems are in general affected by a variety of disturbances on different time scales; high-frequency disturbances, denoted noise, periodic disturbances, referred to as fluctuations, and slow (often monotonic) disturbances, termed drifts. Although a number of procedures frequently are utilized to reduce disturbances, the assessments are still often limited by their residual amounts. Of special importance is that the cavity spacer material is subjected to uncontrolled deformation due to thermal expansion, aging, relaxations, and diffusion of gas into the material that can change its length in an unpredicted manner [1]. This severely limits the performance and usability of FPC-based refractometry.

There are several means to alleviate this. One is to utilize a dual-Fabry–Perot cavity (DFPC) in which two cavities, bored in the same cavity spacer, one serving as the measurement cavity and one as the reference cavity, are simultaneously addressed by two laser fields [1,5,6,10,22–25]. In this case, the shift in the frequency of the laser light can directly be measured as the shift of the beat signal between the two laser fields. An advantage of this is that any change in length of the cavity spacer that affects the two cavities equally does not affect the refractivity assessment. However, since the lengths of two cavities bored

in the same spacer also can fluctuate or drift dissimilarly over time, DFPC-based refractometry will still pick up disturbances from cavity deformation, although often to a significantly lesser extent than when a single FPC is used.

Other means to alleviate the limitations are to construct the DFPC of low thermal expansion glass, e.g., ultralow expansion glass (ULE) [1,24] or Zerodur [2,6–11,13,26–29], place it in a highly temperature stabilized environment (a combined gas and vacuum chamber) [1], and let the system relax and equilibrate for long time periods after each gas filling or emptying process [1]. However, several of these actions are cumbersome to pursue and increase the complexity of the systems. This limits the use of the technology outside well-controlled laboratories.

An alternative is to utilize a methodology that can reduce the influence of disturbances. One such is gas modulation refractometry (GAMOR) [14,15,30–34]. This methodology is built upon two principles, here referred to as two cornerstones; *viz.*, (i) the refractivity of the gas in the measurement cavity is assessed by a frequent referencing of filled measurement cavity beat frequencies to evacuated cavity beat frequencies, and (ii) the evacuated measurement cavity beat frequency at the time of the assessment of the filled measurement cavity beat frequency is estimated by use of an interpolation between two evacuated measurement cavity beat frequency assessments, one performed before and one after the filled cavity assessments. By this, the GAMOR methodology reduces swiftly and conveniently the pickup of various types of disturbances in refractometry systems, not only those from changes in length of the cavity caused by drifts in the temperature of the cavity spacer, but also several of those that have other origins (e.g., those from gas leakages and outgassing) [32,35].

It has been experimentally shown that the GAMOR methodology, when applied to a DFPC refractometry instrumentation utilizing a nontemperature-stabilized cavity spacer made of Zerodur, could reduce the influence of drifts more than 3 orders of magnitude (decreasing the standard deviation from 6.4 Pa to 3.5 mPa) [30]. For pressure assessment in the 5 kPa range, the methodology has demonstrated a sub-parts per million (1σ) precision [31].

The methodology has also opened up for the use of nonconventional cavity-spacer materials; a GAMOR-based system based on an Invar-based DFPC refractometer has recently been realized and characterized [14,33]. It was found that, for a pressure at 4303 Pa, it could provide a minimum deviation of 0.34 mPa [which corresponds to a sub-0.1 ppm relative deviation (or precision)] [14].

This system has, in turn, been used to demonstrate a novel procedure for assessment of cavity deformation [36]. It was shown that the high precision of the instrumentation allows for an assessment of cavity deformation to such a high accuracy that its uncertainty contributes to the uncertainty in the assessment of pressure of N_2 with solely a fraction of the uncertainty of its molar polarizability, presently to a level of a few parts per million [36]. This implies, in practice, that cavity deformation is no longer a limiting factor in GAMOR-based FP refractometer assessments of pressure of N_2.

All these extraordinary achievements originate largely from the ability of the technique to reduce the influence of disturbances, in particular fluctuations and drifts [14,15,30–34]. In fact, as it has recently been scrutinized in some detail [16], the GAMOR methodology has allowed the influence of such disturbances to be reduced to such an extent that the precision plays a virtually insignificant role in the assessment of pressure; the extended uncertainties are dominated by, for one GAMOR system, the uncertainty in the molar polarizability of the gas addressed (for the case with nitrogen, 8 ppm) and, for another (a transportable) system, the assessment of the temperature (26 ppm). Since the assessment of changes of pressure is predominantly given by the precision of the instrumentation, the GAMOR methodology has also significantly increased the capability of refractometer systems to assess changes of pressure.

However, until recently, no detailed analysis of the ability of GAMOR to reduce the pickup of fluctuation and drifts had been given. To remedy this, it was recently explicated how gas modulation can reduce the influence of fluctuations to FP-based systems [32,37]. To continue the scrutiny of the influence of gas modulation on FP-based refractometry, this work reports on the extraordinary ability of modulated refractometry in general, and GAMOR in particular, to reduce the influence of drifts in FP-based refractometry [38]. It does so by providing a comparison (both an estimate based on a theoretical analysis and an experimental assessment) of the abilities of several types of refractometry methodology: unmodulated noninterpolated (UMNI) refractometry [both single-Fabry–Perot cavity (SFPC) refractometry and DFPC refractometry]; unmodulated interpolated (UMI) refractometry; modulated noninterpolated (MNI) refractometry; and modulated interpolated refractometry, here referred to as GAMOR [39].

To quantitatively estimate the extent to which the various methodologies are affected by various types of drifts, we will first, in Section 2, give a short description (using a common nomenclature) of how they assess refractivity, molar density, and pressure. We will then, after various types of drifts are defined, in the Sections 3.B and 3.C, provide a general model of drifts of the frequencies of the cavity modes (and thereby of the beat frequency) during a measurement campaign and assume that they can comprise both linear and nonlinear parts. This will be followed, in Sections 3.D and 3.E, by a description of how the modeled drifts affect the assessment of the shift of the beat frequency in the various methodologies considered. Section 3.F identifies the main origins of the drifts to be: (*i*) drifts of the cavity lengths; and (*ii*) leakages or outgassing into the system. Sections 3.G and 3.H scrutinize (and estimate) the influence of these types of drifts on the assessment of refractivity and pressure by the various types of FPC-based methodologies addressed.

Although it has previously been experimentally demonstrated that GAMOR has an ability to significantly reduce drifts [30], no quantitative comparison of to what extent the various methodologies addressed are affected by different types of drifts has yet been given. To circumvent this shortcoming, additional experimental demonstrations of this are presented here. Following Section 4, which gives information about the experimental setup used, Section 5 therefore provides assessments of the influence of a given number of drifts (deliberately induced under controlled conditions) on the various methodologies addressed. Section 6 provides a summary and conclusions.

Finally, it should be noted that this work deals with the ability to mitigate the influence of drifts on FPC-based refractometry in general and GAMOR in particular. Hence, it mainly addresses the ability to improve on the precision. It also

improves on the accuracy until the precision no longer plays any role in the total uncertainty budget. This ability is of increasing importance the lower the addressed pressure. The uncertainty budget for the GAMOR experimental system used in this work has been presented in a recent work [16].

2. THEORY–MEANS OF ASSESSMENT OF REFRACTIVITY, MOLAR DENSITY, AND PRESSURE IN FPC-BASED REFRACTOMETRY

The modulated FPC-based refractometry methodologies are based on the same fundamental principle as ordinary (unmodulated) (UM) refractometry; they measure the change in refractive index between two situations, with and without gas in the measurement cavity. This implies that they are all governed by the same basic expressions.

A. Assessment of Gas Refractivity from a Measured Shift in Beat Frequency

It has been found convenient to express the refractivity of the gas under scrutiny assessed by FPC-based methodologies as a function of the shift of the beat frequency between the two laser fields probing the two cavities, Δf, and, when mode jumps take place, the shift in mode number of the mode addressed in the measurement cavity, Δq_m, when the latter is filled with (or emptied of) gas [40], as

$$n-1=\frac{\overline{\Delta f}+\overline{\Delta q}_m}{1-\overline{\Delta f}+\varepsilon_m}, \tag{1}$$

where $\overline{\Delta f}$ is the relative shift of the beat frequency given by $\Delta f/\nu_m^{(0)}$, where $\nu_m^{(0)}$ is the evacuated cavity frequency of the measurement laser; and $\overline{\Delta q}_m$ is a shorthand notation for $\Delta q_m/q_m^{(0)}$, where $q_m^{(0)}$ is the number of the mode addressed in the evacuated measurement cavity [31]. ε_m is a refractivity-normalized relative cavity deformation, defined as $(\delta L_m/L_m^{(0)})/(n-1)$, where δL_m and $L_m^{(0)}$ are the change in length of the measurement cavity when it is filled with gas and the length of the measurement cavity when being evacuated, respectively.

The shift in beat frequency between the two laser fields probing the two cavities, Δf, is, in turn, given by

$$\Delta f \equiv f_{(0,g)}-f_{(0,0)}, \tag{2}$$

where $f_{(0,g)}$ and $f_{(0,0)}$ are the beat frequencies assessed when the measurement cavity is filled with gas and evacuated, respectively, which, in turn, are given by

$$\begin{cases} f_{(0,g)} \equiv \nu_r^{(0)}-\nu_m^{(g)} \\ f_{(0,0)} \equiv \nu_r^{(0)}-\nu_m^{(0)}, \end{cases} \tag{3}$$

where $\nu_r^{(0)}$ represents the frequency of the reference laser, which, in this work, for all types of DFPC-based methodologies, is assumed to address an evacuated reference cavity, while it, for SFPC-based refractometry, refers to an external frequency reference. $\nu_m^{(g)}$ and $\nu_m^{(0)}$ are the frequencies of the measurement laser addressing the measurement cavity containing the gas whose properties or amount are to be assessed and when it is evacuated, respectively. A compilation of the nomenclature used is given in Supplement 1. A recipe for how to assess ε_m with an accuracy in the low parts per million range has recently been given [36].

Note that Eq. (1) is valid for all types of refractometry in which the amount of gas in a single FPC is altered, including both UM methodologies (SFPC as well as DFPC refractometry) and modulated ones (MNI refractometry as well as GAMOR) [41].

B. Assessment of Gas Density and Pressure from the Gas Refractivity

The conversion of refractivity, $n-1$, to gas molar density, ρ, is performed through the extended Lorentz–Lorenz equation, given by Eq. (SM-20) in the supplementary material of Ref. [31], which implies that the density can be assessed from the assessed refractivity by

$$\rho=\frac{2}{3A_R}(n-1)\left[1+b_{n-1}(n-1)\right], \tag{4}$$

where A_R and b_{n-1} are the dynamic molar polarizability and a series expansion coefficient, respectively, where the latter is given by $-(1+4B_R/A_R^2)/6$, where, in turn, B_R is the second refractivity virial coefficient in the Lorentz–Lorenz equation for the type of gas addressed [31,35,42,43].

The corresponding pressure, P, can thereafter be obtained from the density as

$$P=RT\rho[1+B_\rho(T)\rho], \tag{5}$$

where R is the ideal gas constant, T is the temperature of the gas, and $B_\rho(T)$ is a density virial coefficient [1,44].

3. MODELING OF DRIFTS OF THE CAVITY MODES AND AN ASSESSMENT OF THEIR INFLUENCE ON VARIOUS TYPES OF FPC-BASED REFRACTOMETRY

Since the assessment of refractivity by the use of FPC-based refractometry methodologies comprises more than one measurement of the measurement cavity mode frequency (when assessed as beat frequencies, $f_{(0,g)}$ and $f_{(0,0)}$), performed at dissimilar time instances (with and without gas in the measurement cavity), and the beat frequency depends on several properties of the system used, a refractivity assessment will be affected by the drifts that take place in the system between the time instances of the individual assessments.

Since the leading term of Eq. (1) for the refractivity is $\Delta f/\nu_m^{(0)}$, and the relative drift in $\nu_m^{(0)}$ over any appreciable amount of time is significantly smaller than that of Δf, the error (or uncertainty) in the assessed refractivity, denoted $\delta(n-1)$, can be assessed as $\delta[\Delta f]/\nu_m^{(0)}$, where $\delta[\Delta f]$ represents the error (or uncertainty) in the assessment of the shift in the beat frequency from drifts that take place when the measurement cavity is filled from vacuum to the pressure to be assessed (i.e., in Δf).

A. Types of Drift

Although both cornerstones upon which the GAMOR methodology relies contribute to a reduction of the influence of drifts, they do not do so to the same extent for all types of drifts. It

is therefore of importance to distinguish between those that affect the cavity mode frequencies persistently and continuously during the entire measurement campaign, irrespective of the state of the gas modulation cycle, here referred to as **campaign-persistent drifts** (for simplicity denoted drifts of **Type I**), from those that are reset once per gas modulation cycle by the gas evacuation process (so the drift process starts over for each modulation cycle), here referred to as **cycle-limited drifts** (referred to as drifts of **Type II**). The Type II drifts, in turn, are separated into two subcategories, *viz.*, **(a)** those that affect the refractivity of the gas in the reference cavity and **(b)** those that affect the refractivity in the measurement cavity. Drifts of the physical lengths of the cavities are thus drifts of Type I. Leakages and outgassing into the reference cavity represent drifts of Type I for the case the reference cavity is sealed off during the entire measurement campaign while they constitute drifts of Type IIa for the case the reference cavity is evacuated once per gas modulation cycle. Leakages or outgassing into the measurement cavity are of Type IIb.

B. Model for the Drifts of the Evacuated Cavity Mode Frequencies

Since drifts represent disturbances that take place on long time scales [38], it is possible to model the error (or uncertainty) of the shift in the beat frequency due to drifts in terms of a Taylor expansion. To do this in an as general manner as possible, we will assume that the evacuated cavity mode frequency for each cavity i (where $i = m$ or r, representing the measurement and the reference cavity, respectively) and for each gas filling-and-emptying process (or gas modulation cycle), $\nu_i^{(0)}(t)$, can be written as a Taylor series expanded around the time instance when the filled measurement cavity assessment, $f_{(0,g)}$, is made, which is at t_g, as

$$\nu_i^{(0)}(t) = \nu_i^{(0)}(t_g) + \left(\frac{\partial \nu_i^{(0)}}{\partial t}\right)_{t_g}(t - t_g) + \frac{1}{2}\left(\frac{\partial^2 \nu_i^{(0)}}{\partial t^2}\right)_{t_g}(t - t_g)^2 + O[(t - t_g)^3], \quad (6)$$

where $(\partial \nu_i^{(0)}/\partial t)_{t_g}$ and $(\partial^2 \nu_i^{(0)}/\partial t^2)_{t_g}$ are the first- and second-order derivatives of the frequency of the cavity mode addressed in the evacuated cavity i with respect to time at t_g, representing the linear and first-order nonlinear drift rates, respectively. The $O[(t - t_g)^3]$–term denotes the sum of all higher-order contributions in the Taylor series expansion, which, close to the center point of the expansion (i.e., for small values of $t - t_g$), becomes the least significant term (often negligible).

C. Corresponding Drifts of the Evacuated Measurement Cavity Beat Frequency

If the frequencies of the cavity modes drift, the beat frequencies, i.e., $f_{(0,g)}$ and $f_{(0,0)}$, will also drift. Equation (3) indicates that, if the evacuated cavity mode frequencies have time dependences according to Eq. (6), the evacuated measurement cavity beat frequency, $f_{(0,0)}(t)$, can be expressed as

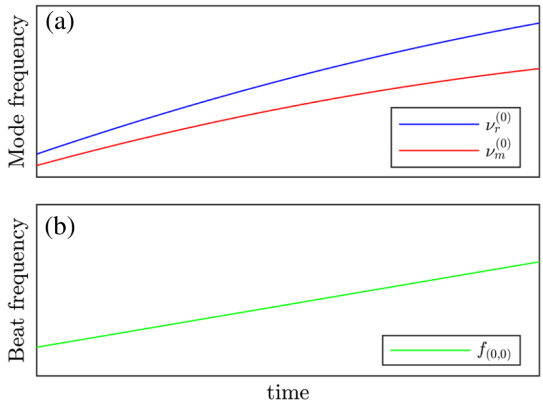

Fig. 1. Schematic illustration of possible drifts of the evacuated cavity mode frequencies and the corresponding beat frequency. (a) Evacuated cavity mode frequencies of the modes addressed in the two cavities exposed to drifts, $\nu_r^{(0)}(t)$ and $\nu_m^{(0)}(t)$, given by Eq. (6); (b) corresponding evacuated measurement cavity beat frequency, $f_{(0,0)}(t)$, representing their difference, given by Eq. (7).

$$f_{(0,0)}(t) = f_{(0,0)}(t_g) + \left(\frac{\partial f_{(0,0)}}{\partial t}\right)_{t_g}(t - t_g) + \frac{1}{2}\left(\frac{\partial^2 f_{(0,0)}}{\partial t^2}\right)_{t_g}(t - t_g)^2 + O[(t - t_g)^3], \quad (7)$$

where

$$f_{(0,0)}(t_g) = \nu_r^{(0)}(t_g) - \nu_m^{(0)}(t_g)$$

$$\left(\frac{\partial f_{(0,0)}}{\partial t}\right)_{t_g} = \left(\frac{\partial \nu_r^{(0)}}{\partial t}\right)_{t_g} - \left(\frac{\partial \nu_m^{(0)}}{\partial t}\right)_{t_g}$$

$$\left(\frac{\partial^2 f_{(0,0)}}{\partial t^2}\right)_{t_g} = \left(\frac{\partial^2 \nu_r^{(0)}}{\partial t^2}\right)_{t_g} - \left(\frac{\partial^2 \nu_m^{(0)}}{\partial t^2}\right)_{t_g}. \quad (8)$$

An example of this is given in Fig. 1. The frequencies of the cavity modes of the two evacuated cavities, $\nu_r^{(0)}(t)$ and $\nu_m^{(0)}(t)$, when exposed to both linear and nonlinear drifts according to Eq. (6) [in this case with $(\partial \nu_i^{(0)}/\partial t)_{t_g} > 0$ and $(\partial^2 \nu_i^{(0)}/\partial t^2)_{t_g} < 0$], are schematically illustrated by the two curves in panel (a), while the corresponding evacuated measurement cavity beat frequency, $f_{(0,0)}(t)$, given by their difference, i.e., by Eq. (7), is given by the green solid curve in panel (b).

By incorporating a sufficient number of terms in the Taylor series in Eqs. (6) and (7), it is possible to make $\nu_i^{(0)}(t)$ and $f_{(0,0)}(t)$ arbitrarily accurate representations of the drifts of the evacuated mode frequencies and the evacuated measurement cavity beat frequency, respectively.

D. Influence of the Modeled Drifts of the Evacuated Measurement Cavity Beat Frequency on the Assessment of the Shift of the Beat Frequency in Various Types of FPC-Based Methodologies

In refractometry, to allow thermal equilibration to take place in the system (which, for some types of systems, in particular those with large gas volumes, for which the pV work performed

by the gas is substantial [45], and with significant heat islands [46], can take substantial amount of time), the evacuated and filled measurement cavity assessments are often well separated in time from each other (often with time separations of days, from time to time with even longer separations). Although common measurement procedures generally prescribe repeated measurements of any assessed quantity, it is not customary to do so in refractometry, since this would take even longer time spans. We will consider this and, when solely a single gas filling and evacuation process is performed during a given measurement campaign, we will here refer to it as UM refractometry.

Moreover, as is shown below, although it is also advantageous to perform an evacuated measurement cavity assessment more than once per campaign, not all refractometry protocols prescribe such a procedure. When UM refractometry is performed with only one evacuated measurement cavity assessment, it will henceforth be referred to as UMNI refractometry. When more than one evacuated measurement cavity assessment is performed during a measurement campaign, it is possible to perform interpolation between consecutive such assessments. When such a procedure is used together with UM refractometry, it will henceforth be referred to as **UMI** refractometry.

When more than one filling and evacuation of the measurement cavity assessment is performed during a measurement campaign, the procedure will here be referred to as modulated refractometry. Similar to the case with UM refractometry, when this is performed, it can be performed either without or with interpolation between such consecutive assessments. When performed without, it will be referred to as **MNI** refractometry; while when performed with interpolation, i.e., when modulated interpolated refractometry is performed, it will be referred to as **GAMOR**.

Largely depending on the construction of the system, all four types of methodologies have been used (and are used) in various ways in laboratories worldwide. To allow for a comparison of the relative advantages of the various types of methodologies, and an estimate of their abilities to reduce the pick-up of drifts, all these methodologies (UMNI, UMI, MNI, and GAMOR) will below be described, scrutinized, and compared in some detail.

1. Noninterpolated Refractometry

To allow for a comparison between various types of methodologies, we will initially, irrespective of whether we deal with UM or modulated refractometry, assume that the evacuated and the filled measurement cavity assessments take place at the time instances t_n and t_g, respectively (where $t_g > t_n$). This implies that noninterpolated (NI) methodologies assess the shift in beat frequency as expressed by Eq. (2), as

$$\Delta f(t_n, t_g) = f_{(0,g)}(t_g) - f_{(0,0)}(t_n). \tag{9}$$

However, due to drifts, this shift will differ from the (ideal) beat frequency shift that should be used in Eq. (1) if a drift-free assessment should be performed, which would take place if $f_{(0,g)}$ and $f_{(0,0)}$ would be assessed at the same time instance, denoted $\Delta f(t_g, t_g)$. For the case when the drifts are either of Type I or IIa (i.e., when the drifts do not affect the gas in the measurement cavity), this is defined as

$$\Delta f(t_g, t_g) = f_{(0,g)}(t_g) - f_{(0,0)}(t_g). \tag{10}$$

Use of Eq. (9) for assessment of the beat frequency therefore gives rise to an error in the assessments.

For these types of drifts, this error, denoted $\delta[\Delta f(t_n, t_g)]$, is given by the difference between these two shifts, i.e., $\Delta f(t_n, t_g) - \Delta f(t_g, t_g)$. Making use of Eqs. (9) and (10) implies that this error can, for the NI methodologies, be written as

$$\delta[\Delta f(t_n, t_g)] = f_{(0,0)}(t_g) - f_{(0,0)}(t_n). \tag{11}$$

This shows that, when such methodologies are used, the error (or uncertainty) in the shift in beat frequency, $\delta[\Delta f]$, which produces an error (or uncertainty) in the assessed refractivity, $\delta(n-1)$, of $\delta[\Delta f]/\nu_m^{(0)}$, can, for drifts that are either of Type I or IIa, be represented by the difference between the evacuated measurement cavity beat frequencies $f_{(0,0)}(t)$ at t_g and t_n [47].

Note that while $f_{(0,0)}(t_n)$ in Eq. (11) is the accessible and measured evacuated measurement cavity beat frequency assessed at t_n, $f_{(0,0)}(t_g)$ represents the actual (but nonmeasurable) evacuated measurement cavity beat frequency when the measurement cavity is filled with gas, i.e., at t_g. To estimate $\delta[\Delta f(t_n, t_g)]$, it is therefore of importance to consider possible time developments of the evacuated measurement cavity beat frequency in the presence of drifts, i.e., $f_{(0,0)}(t)$.

A possible such drift, given for a single filling-and-emptying process (or a single gas modulation cycle) by Eq. (7), which is schematically shown in Fig. 1(b), is illustrated in more detail by the blue solid curve (the uppermost curve in the center of the graph) in Fig. 2. While the latter of the two evacuated cavity measurement beat frequencies in Eq. (11), i.e., $f_{(0,0)}(t_n)$, is represented by the leftmost cross in Fig. 2, the former, i.e., $f_{(0,0)}(t_g)$, is indicated by the red circle. Making use of Eq. (7) for the evacuated measurement cavity beat frequency at t_n, Eq. (11) indicates that the error (or uncertainty) in the shift of the beat frequency from drifts of either Type I or IIa that appears in assessments performed by NI refractometry, $\delta[\Delta f(t_n, t_g)]$, can be written swiftly.

UMNI refractometry: For the UMNI methodology (for which the evacuated measurement cavity assessment is performed at a time instance $t_n = 0$), this can be written as

$$\delta[\Delta f(t_n = 0, t_g)] = \left(\frac{\partial f_{(0,0)}}{\partial t}\right)_{t_g} t_g - \frac{1}{2}\left(\frac{\partial^2 f_{(0,0)}}{\partial t^2}\right)_{t_g} t_g^2 + O[t_g^3]. \tag{12}$$

MNI refractometry: For the MNI methodology, the same expression can, for modulation cycle n, be written as

$$\delta[\Delta f(t_n, t_g)] = \left(\frac{\partial f_{(0,0)}}{\partial t}\right)_{t_g} (t_g - t_n) - \frac{1}{2}\left(\frac{\partial^2 f_{(0,0)}}{\partial t^2}\right)_{t_g} (t_g - t_n)^2 + O[(t_g - t_n)^3]. \tag{13}$$

2. Interpolated Refractometry

UMI refractometry: When UM refractometry is performed, it is often possible to make one evacuated measurement cavity

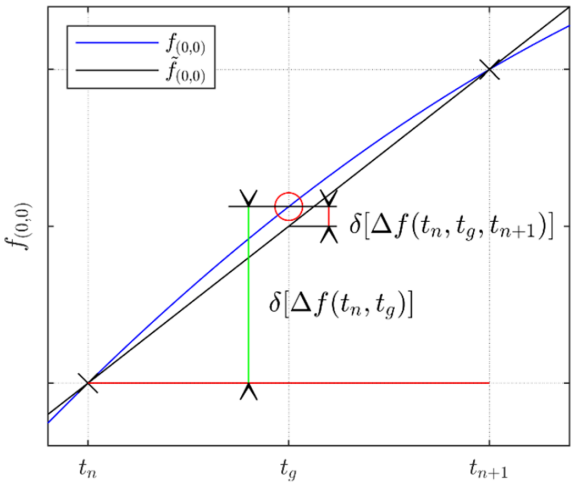

Fig. 2. Blue solid curve (the uppermost in the center of the graph): the evacuated measurement cavity beat frequency for modulated refractometry in the presence of drifts, $f_{(0,0)}(t)$, as given by Eq. (7) (for a case with $(\partial f_{(0,0)}/\partial t)_{t_g} > 0$ and $(\partial^2 f_{(0,0)}/\partial t^2)_{t_g} < 0$). The beat frequency at time t_g, at which the gas measurement is performed, denoted $f_{(0,0)}(t_g)$, is marked by a red circle. The beat frequency measured at time t_n, $f_{(0,0)}(t_n)$, is marked by the leftmost cross (×). Both NI methodologies (i.e., UMNI and MNI) consider $f_{(0,0)}(t_n)$ to be an appropriate representation of $f_{(0,0)}$ for the entire gas filling-and-emptying process (or gas modulation cycle), respectively, represented by the red horizontal line (the lowermost in the center of the graph). The long (leftmost) green vertical line, denoted $\delta[\Delta f(t_n, t_g)]$ and defined by Eq. (13), illustrates, for drifts of Type I or IIa, the error in the assessment of the beat frequency for both these methodologies, mainly given by either of Eq. (20), (21), or (22). The slanted black straight line represents the estimated evacuated measurement cavity beat frequency, $\tilde{f}_{(0,0)}(t_n, t, t_{n+1})$, created by a linear interpolation between two evacuated measurement cavity beat frequency assessments (marked by the two crosses, ×) when either of the interpolated methodologies (UMI or GAMOR) is used [according to Eq. (12) or (13), respectively] with an instrumentation affected by drifts of Type I (the case with UMI refractometry is illustrated by the figure with $t_n = 0$ and $t_{n+1} = t_{\text{cmp}}$). The short (rightmost) red vertical line, denoted $\delta[\Delta f(t_n, t_g, t_{n+1})]$ and defined either by Eq. (16) or (19), illustrates the error (or uncertainty) in the assessment of the beat frequency made when the GAMOR methodology is used in an instrumentation exposed to such types of drifts. Note that, for a well-constructed refractometry system, dominated by slow drifts, and, in particular, when modulation (with short modulation cycles) is used, the curvature of $f_{(0,0)}(t)$ in the figure is, for illustrative purposes, greatly exaggerated. In such cases, the residual error (or uncertainty) when GAMOR is applied (the vertical red arrow) can be significantly smaller than what is schematically illustrated in the figure.

assessment at the start of the measurement campaign and one at its end. Assuming that the first takes place at a time 0, and denoting the time instance for the latter t_{cmp}, the interpolated evacuated measurement cavity assessment for UMI refractometry can be assessed, for all time instances during the measurement campaign, i.e., for $0 \le t \le t_{\text{cmp}}$, as

$$\tilde{f}_{(0,0)}(t, t_{\text{cmp}}) = f_{(0,0)}(0) + \frac{f_{(0,0)}(t_{\text{cmp}}) - f_{(0,0)}(0)}{t_{\text{cmp}}} t. \quad \textbf{(14)}$$

By subtracting this interpolated evacuated measurement cavity beat frequency at the time of the assessment of the filled measurement cavity beat frequency (i.e., at t_g), $\tilde{f}_{(0,0)}(t_g, t_{\text{cmp}})$, from the measured (drift-influenced) beat frequency during gas filling, $f_{(0,g)}(t_g)$, a Type I drift-corrected net beat frequency, denoted $\Delta f_{\text{UMI}}(t_g)$, results. This entity represents the Δf to be used in Eq. (1) when UMI is performed.

In this case, the error in the assessment of the evacuated measurement cavity beat frequency (performed at t_g), now denoted $\delta[\Delta f(t_g, t_{\text{cmp}})]_{\text{UMI}}$, is no longer given by Eq. (11), but rather, by

$$\delta[\Delta f(t_g, t_{\text{cmp}})]_{\text{UMI}} = f_{(0,0)}(t_g) - \tilde{f}_{(0,0)}(t_g, t_{\text{cmp}}). \quad \textbf{(15)}$$

For Type I drifts (i.e., drifts of the lengths of the cavities and, for the case when the reference cavity is sealed-off during the entire measurement campaign, leakages and outgassing into this cavity), for which the evacuated cavity mode frequencies are continuous functions of time also outside the range of a single filling-and-emptying process (or gas modulation cycle) [48], the interpolation process will reduce the errors (uncertainties) of the beat frequency. For this type of drift, for which $\tilde{f}_{(0,0)}(t_g, t_{\text{cmp}})$ is schematically represented by the slanted black line in Fig. 2, and when UMI is performed, the leading term of the error (or uncertainty) in the assessment of the shift of the evacuated measurement cavity beat frequency [obtained by use of Eqs. (7), (14), and (15)] is given by

$$\delta[\Delta f(0, t_g, t_{\text{cmp}})]_{\text{UMI}} = -\frac{1}{2}\left[\left(\frac{\partial^2 f_{(0,0)}}{\partial t^2}\right)_{t_g}\right]_I t_g^2, \quad \textbf{(16)}$$

where the subscript $_I$ indicates that the drifts are of Type I.

GAMOR: As was alluded to above, the GAMOR methodology can be described as a combination of two cornerstones, *viz.*, a frequent referencing of filled measurement cavity beat frequencies to evacuated cavity beat frequencies and, to assess the evacuated measurement cavity beat frequency at the time of the assessment of the filled measurement cavity beat frequency, the use of an interpolation between two evacuated measurement cavity beat frequency assessments, one performed before and one after the filled cavity assessments. To clarify the role of the two cornerstones on the ability of the methodology to reduce the pickup of drifts, the principles of GAMOR performed on an experimental system exposed to drifts of Type I, i.e., campaign-persistent drifts, are schematically illustrated in Fig. 3.

Panel (a) illustrates the pressure in the measurement cavity, which, according to cornerstone (*i*), is alternately evacuated and filled with gas (upper red curve) while the reference cavity is held at a constant pressure (in this case for simplicity chosen to be at vacuum, lower blue curve). This implies that the influence of drifts, which, in general, affect the frequencies of both the measurement and the reference lasers [although possibly to dissimilar extent, as shown in panel (b)], and thereby the assessed beat frequency [the upper black curve in panel (c)], can be reduced by shortening the modulation cycle period; for a given drift rate, the shorter the gas modulation cycle time is, the less will the assessed beat frequency be affected by drifts [49].

In addition, according to cornerstone (*ii*), the evacuated measurement cavity beat frequency is estimated by the use of a linear interpolation between two evacuated measurement cavity beat frequency assessments performed in rapid succession—for

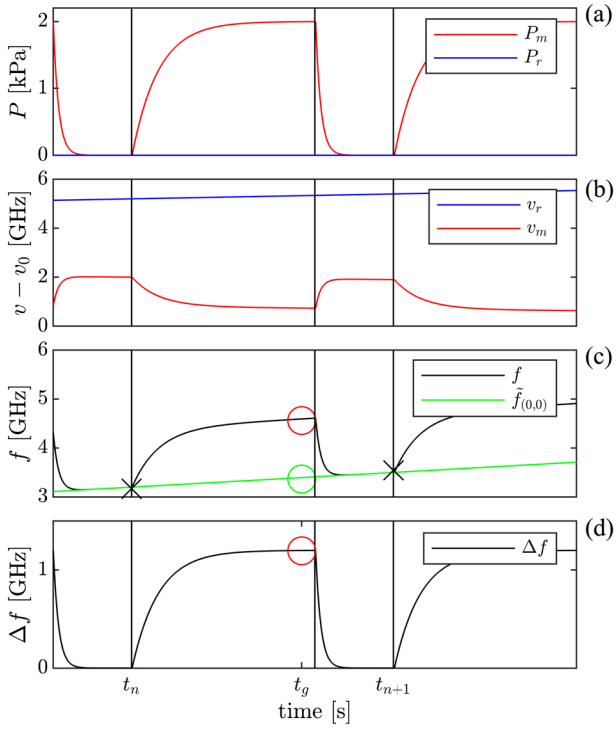

Fig. 3. Illustration of the principles of GAMOR on an experimental system exposed to drifts of Type I, i.e., campaign-persistent drifts, displayed over two full modulation cycles. (a) displays, as functions of time, the pressures in the measurement cavity, $P_m(t)$, (the upper red curve) and in the reference cavity, $P_r(t)$, (the lower blue curve). (b) shows the corresponding frequencies of the measurement and reference lasers, $\nu_m(t)$ (the lower red curve) and $\nu_r(t)$ (the upper blue curve), respectively, in the presence of drifts (for display purposes, in the absence of mode jumps and offset to a common frequency ν_0). (c) illustrates the corresponding beat frequencies: by the upper black curve, the measured one in the presence of the gas modulation, $f_{(0,g)}(t)$, and, by the lower green line, the estimated evacuated measurement cavity beat frequency, $\tilde{f}_{(0,0)}(t_n, t, t_{n+1})$, which, according to Eq. (17), has been constructed as a linear interpolation between two evacuated measurement cavity assessments (taken at the positions of the crosses). (d), finally, displays, by the black curve, the drift-corrected shift in beat frequency, $\Delta f_G(t)$, at each time instance given by the difference between the beat frequency measured with gas in the measurement cavity, $f_{(0,g)}(t)$, and the (intercycle) interpolated evacuated measurement cavity beat frequency, $\tilde{f}_{(0,0)}(t_n, t, t_{n+1})$. The circles in the two lowermost panels illustrate the parts of the data that are used for evaluation of the gas refractivity; the red and the green circles in (c) represent $f_{(0,g)}(t_g)$ and $\tilde{f}_{(0,0)}(t_n, t_g, t_{n+1})$, respectively, while the red circle in (d) corresponds to their difference, i.e., $\Delta f_G(t_g)$. The drifts and the slope of the interpolated evacuated measurement cavity beat frequency have been greatly exaggerated for display purposes.

cycle n, one performed at a time t_n, denoted $f_{(0,0)}(t_n)$, and the other a time t_{n+1}, denoted $f_{(0,0)}(t_{n+1})$, both marked by crosses in Fig. 3(c). By this intercycle interpolation, the evacuated measurement cavity beat frequency can be estimated at all times t during a modulation cycle. For cycle n, for which $t_n \le t \le t_{n+1}$, it is estimated as

$$\tilde{f}_{(0,0)}(t_n, t, t_{n+1}) = f_{(0,0)}(t_n) + \frac{f_{(0,0)}(t_{n+1}) - f_{(0,0)}(t_n)}{t_{n+1} - t_n}(t - t_n). \quad \textbf{(17)}$$

For the case with drifts of Type I, this (intercycle) interpolated value is represented by the green line in Fig. 3(c). The value of the estimated evacuated measurement cavity beat frequency at the time when the filled measurement cavity assessment is performed, denoted $\tilde{f}_{(0,0)}(t_n, t_g, t_{n+1})$, is marked by a green circle.

Similar to the case with UMI refractometry, by subtracting the estimated (interpolated) evacuated measurement cavity beat frequency [$\tilde{f}_{(0,0)}(t_n, t, t_{n+1})$, the green line] from the measured (drift-influenced) beat frequency during gas filling [$f_{(0,g)}(t)$, the black curve], both in panel (c), an intercycle Type I drift-corrected net beat frequency, denoted $\Delta f_G(t)$ and represented by the black curve in panel (d), results. The value of this curve at t_g, i.e., $\Delta f_G(t_g)$, represents the Δf to be used in Eq. (1) when GAMOR is performed [50].

In this case, the error in the assessment of the evacuated measurement cavity beat frequency (performed at t_g), now denoted $\delta[\Delta f(t_n, t_g, t_{n+1})]_G$, is given by

$$\delta[\Delta f(t_n, t_g, t_{n+1})]_G = f_{(0,0)}(t_g) - \tilde{f}_{(0,0)}(t_n, t_g, t_{n+1}). \quad \textbf{(18)}$$

Again, for Type I drifts, the interpolation process can reduce the errors (uncertainties) of the beat frequency. For this type of drift, for which $\tilde{f}_{(0,0)}(t_n, t_g, t_{n+1})$ is schematically represented by the slanted black line in Fig. 2, the leading term of the error (or uncertainty) in the assessment of the shift of the evacuated measurement cavity beat frequency [obtained by use of Eqs. (7), (17), and (18)] is given by

$$\delta[\Delta f(t_n, t_g, t_{n+1})]_G = -\frac{1}{2}\left[\left(\frac{\partial^2 f_{(0,0)}}{\partial t^2}\right)_{t_g}\right]_I (t_g - t_n)^2. \quad \textbf{(19)}$$

This entity is schematically illustrated by the short (rightmost) red vertical line in Fig. 2, denoted $\delta[\Delta f(t_n, t_g, t_{n+1})]$. This shows that the effect of cornerstone (*ii*) on drifts of Type I is to eliminate the dependence of its linear part. Together with the modulation process that forms one part of the GAMOR principle, this has a profound effect on the resilience to drifts of Type I.

E. Influence of the Length of the Gas Filling and Emptying Cycle on the Assessment of the Shift of the Beat Frequency in Various Types of Methodologies

To estimate the role of, on the one hand, the modulation procedure, and on the other hand, the interpolation process, it is convenient to rewrite the above expressions in terms of the length of the gas filling and emptying cycle, which, for the UM methodologies, for simplicity, is assumed to be given by the length of the measurement campaign, t_{cmp}, while for the modulated ones, it is given by $t_{n+1} - t_n$, henceforth denoted t_{mod}. To assess the influence of drifts of the cavity lengths, leakages, and outgassing into the cavities, it is convenient to also express the expressions for the errors (or uncertainties) in the assessment of the shift of the evacuated measurement cavity beat frequency in terms of the individual frequencies of the modes of the evacuated cavities, i.e., $\nu_r^{(0)}(t)$ and $\nu_m^{(0)}(t)$ for the various methodologies addressed.

1. UMNI Refractometry

SFPC-based refractometry: For the case when SFPC-based refractometry is performed, the reference laser is not stabilized with respect to any reference cavity bored in the same spacer block as the measurement cavity; it is instead stabilized by some other (external) means. Its frequency will therefore not be affected by any drift influencing the cavities. Under the assumption that this external stabilization is adequate, i.e., that $\nu_r^{(0)}(t) = \nu_r^{(0)}(t_g) = \nu_r^{(0)}(t_n)$ under the entire measurement campaign, this implies that, for any drift that can be expressed by the Taylor series expansion given in Eq. (6) (i.e., from drifts of Type I or IIa), the leading term of the error (or uncertainty) in the assessment of the shift of the beat frequency for SFPC-based refractometry when UMNI is performed, $\delta[\Delta f(t_{\mathrm{cmp}})]_{\mathrm{UMNI}}^{\mathrm{SFPC}}$, can be written, by the use of Eqs. (8) and (12), as

$$\delta[\Delta f(t_{\mathrm{cmp}})]_{\mathrm{UMNI}}^{\mathrm{SFPC}} = -\zeta_{\mathrm{UM}}\left(\frac{\partial \nu_m^{(0)}}{\partial t}\right)_{t_g} t_{\mathrm{cmp}}, \tag{20}$$

where ζ_{UM} represents the fraction of the entire campaign into which the filled measurement cavity assessment is performed, defined as t_g/t_{cmp}.

This shows that the error (or uncertainty) in conventional SFPC-based UMNI refractometry is predominantly given by a product of the first-order derivative of the frequency of the mode addressed in the evacuated measurement cavity (its linear drift rate), $(\partial \nu_m^{(0)}/\partial t)_{t_g}$, and the separation in time between the assessments of the two beat frequencies $[f_{(0,0)}(0)$ and $f_{(0,g)}(t_g)]$, here expressed as $\zeta_{\mathrm{UM}} t_{\mathrm{cmp}}$. This error (or uncertainty) is illustrated by the long (leftmost) green vertical line, for generality denoted $\delta[\Delta f(t_n, t_g)]$, in Fig. 2.

DFPC-based refractometry: For the case when DFPC-based UMNI refractometry is performed, the reference laser is addressing a reference cavity bored in the same spacer block as the measurement cavity and is therefore likewise exposed to drifts. Again, making use of Eqs. (8) and (12) implies that the leading term of the error (or uncertainty) in the assessment of the beat frequency in DFPC-based UMNI refractometry, $\delta[\Delta f(t_{\mathrm{cmp}})]_{\mathrm{UMNI}}^{\mathrm{DFPC}}$, can be written as

$$\delta[\Delta f(t_{\mathrm{cmp}})]_{\mathrm{UMNI}}^{\mathrm{DFPC}} = \zeta_{\mathrm{UM}}\left[\left(\frac{\partial \nu_r^{(0)}}{\partial t}\right)_{t_g} - \left(\frac{\partial \nu_m^{(0)}}{\partial t}\right)_{t_g}\right] t_{\mathrm{cmp}}. \tag{21}$$

This shows that in conventional DFPC-based UMNI refractometry, the error from drifts of Type I or IIa is primarily given by a product of the *difference* between the first-order derivatives of the frequency of the mode addressed in the evacuated cavities, $(\partial \nu_r^{(0)}/\partial t)_{t_g} - (\partial \nu_m^{(0)}/\partial t)_{t_g}$, (i.e., the difference in linear drift rates of the two cavities), and the separation in time between the $f_{(0,g)}$ and $f_{(0,0)}$ assessments, i.e., $\zeta_{\mathrm{UM}} t_{\mathrm{cmp}}$. Also, this error (or uncertainty) is schematically illustrated by the long (leftmost) green vertical line denoted $\delta[\Delta f(t_n, t_g)]$ in Fig. 2.

2. MNI Refractometry

When modulation is used without interpolation, i.e., when MNI refractometry is performed, the methodology provides an assessment of the beat frequency with an error (or uncertainty), $\delta[\Delta f(t_{\mathrm{mod}})]_{\mathrm{MNI}}$, that has a form similar to that for DFPC-based UMNI refractometry, Eq. (21), that, according to Eq. (13), most conveniently can be written as

$$\delta[\Delta f(t_{\mathrm{mod}})]_{\mathrm{MNI}} = \zeta_M\left[\left(\frac{\partial \nu_r^{(0)}}{\partial t}\right)_{t_g} - \left(\frac{\partial \nu_m^{(0)}}{\partial t}\right)_{t_g}\right] t_{\mathrm{mod}}, \tag{22}$$

where ζ_M represents the fraction of the gas modulation cycle, t_{mod}, into which the filled measurement cavity assessment is performed, defined as $(t_g - t_n)/t_{\mathrm{mod}}$.

However, although of similar form, Eqs. (22) and (21) differ by the fact that the length of the gas modulation cycle for MNI refractometry, t_{mod}, is significantly shorter (often orders of magnitude) than the time separation between the assessments of $f_{(0,g)}$ and $f_{(0,0)}$ in the UM case, i.e., t_{cmp}. This indicates that MNI refractometry is significantly less affected by drifts of the evacuated cavity modes than UMNI refractometry.

3. UMI Refractometry

When UM refractometry is used with interpolation, which predominantly takes place in systems in which it takes a substantial amount of time to reach thermal equilibration (primarily those with large gas volumes and pronounced heat islands), i.e., when UMI is performed, in systems in which there are drifts of Type I, Eqs. (8) and (16) indicate that the leading term of the error (or uncertainty) in the assessment of the shift of the evacuated measurement cavity beat frequency is given by

$$\delta[\Delta f(t_{\mathrm{cmp}})]_{\mathrm{UMI}} = -\frac{\zeta_{\mathrm{UM}}(1-\zeta_{\mathrm{UM}})}{2}\left[\left(\frac{\partial^2 \nu_r^{(0)}}{\partial t^2}\right)_{t_g} - \left(\frac{\partial^2 \nu_m^{(0)}}{\partial t^2}\right)_{t_g}\right]_I t_{\mathrm{cmp}}^2, \tag{23}$$

where the subscript $_I$ indicates that the drifts are of Type I.

4. GAMOR

When modulated refractometry is used with interpolation, i.e., when GAMOR is performed, which can be the case in systems in which thermal equilibration swiftly (on the time scale of seconds) is reached (primarily those with small gas volumes and no heat islands) [51], and for the case when the system is affected by drifts of Type I, Eq. (19) indicates that the leading term of the error (or uncertainty) in the assessment of the shift of the evacuated measurement cavity beat frequency is given by

$$\delta[\Delta f(t_{\mathrm{mod}})]_G = -\frac{\zeta_M(1-\zeta_M)}{2}\left[\left(\frac{\partial^2 \nu_r^{(0)}}{\partial t^2}\right)_{t_g} - \left(\frac{\partial^2 \nu_m^{(0)}}{\partial t^2}\right)_{t_g}\right]_I t_{\mathrm{mod}}^2. \tag{24}$$

As for the NI cases, although Eqs. (23) and (24) are of similar form, they differ by the fact that the length of the gas modulation cycle for GAMOR, t_{mod}, is significantly shorter than the time separation between the assessments of $f_{(0,g)}$ and $f_{(0,0)}$ in

the UM case, i.e., t_{cmp}. This indicates that GAMOR refractometry is significantly less affected by drifts of the evacuated cavity modes than UMI refractometry.

5. Interpolated Refractometry in the Presence of Drifts of Type IIa

In both interpolated methodologies (i.e., UMI and GAMOR), the interpolations given by Eqs. (14) and (17) do not have any effect on cycle-limited drifts (i.e., drifts of Type II), since for these $f_{(0,0)}(t_{\mathrm{cmp}}) = f_{(0,0)}(0)$ and $f_{(0,0)}(t_{n+1}) = f_{(0,0)}(t_n)$, whereby $\tilde{f}_{(0,0)}(t_{\mathrm{cmp}}, t_{\mathrm{cmp}}) = f_{(0,0)}(0)$ and $\tilde{f}_{(0,0)}(t_n, t_{n+1}, t_{n+1}) = f_{(0,0)}(t_n)$, which in turn implies that Eqs. (15) and (18) revert to Eq. (11). This implies that the errors (or uncertainties) in the assessment of the shift of the beat frequency from such drifts of the evacuated measurement cavity modes by the UMI and GAMOR methodologies are given by the expressions of the error (or uncertainty) in the assessment of the shift of the beat frequency of the corresponding NI methodologies (UMNI and MNI refractometry), i.e., Eqs. (21) and (22). Hence, when drifts of both Type I and IIa are present simultaneously, the errors (or uncertainties) in the shift of the beat frequency are, when interpolation is applied, for the case with UMI, given by a combination of Eqs. (21) and (23), *viz.*,

$$\begin{aligned}\delta[\Delta f(t_{\mathrm{cmp}})]_{\mathrm{UMI}} &= \zeta_{\mathrm{UM}}\left[\left(\frac{\partial \nu_r^{(0)}}{\partial t}\right)_{t_g} - \left(\frac{\partial \nu_m^{(0)}}{\partial t}\right)_{t_g}\right]_{\mathrm{IIa}} t_{\mathrm{cmp}} \\ &\quad - \frac{\zeta_{\mathrm{UM}}(1-\zeta_{\mathrm{UM}})}{2}\left[\left(\frac{\partial^2 \nu_r^{(0)}}{\partial t^2}\right)_{t_g} - \left(\frac{\partial^2 \nu_m^{(0)}}{\partial t^2}\right)_{t_g}\right]_{I} t_{\mathrm{cmp}}^2,\end{aligned} \tag{25}$$

while for the case with GAMOR, they are given by a combination of Eqs. (22) and (24), i.e.,

$$\begin{aligned}\delta[\Delta f(t_{\mathrm{mod}})]_{G} &= \zeta_{M}\left[\left(\frac{\partial \nu_r^{(0)}}{\partial t}\right)_{t_g} - \left(\frac{\partial \nu_m^{(0)}}{\partial t}\right)_{t_g}\right]_{\mathrm{IIa}} t_{\mathrm{mod}} \\ &\quad - \frac{\zeta_{M}(1-\zeta_{M})}{2}\left[\left(\frac{\partial^2 \nu_r^{(0)}}{\partial t^2}\right)_{t_g} - \left(\frac{\partial^2 \nu_m^{(0)}}{\partial t^2}\right)_{t_g}\right]_{I} t_{\mathrm{mod}}^2.\end{aligned} \tag{26}$$

Here, the first terms (marked with subscript $_{\mathrm{IIa}}$) represent the drifts in the frequency of the mode addressed from drifts of Type IIa (primarily drifts due to leakages and outgassing in the reference cavity if evacuated once per gas modulation cycle; see below) while the second term denotes drifts of Type I (predominantly drifts in the physical lengths of the cavities, and, for the case when the reference cavity is sealed off during the entire measurement campaign, drifts from leakages and outgassing in this cavity).

This shows that although the interpolated methodologies have an ability to reduce the influence of drifts of both Type I and IIa (with respect to the UM methodologies), they simultaneously have an ability to reduce the effect of drifts of Type I significantly more than those of Type IIa. However, as was alluded to above, since t_{mod} is significantly shorter than t_{cmp}, they do so to dissimilar degrees.

F. Origin of Drifts of the Evacuated Cavity Mode Frequencies

As was alluded to above, the main origins of drifts of the assessed evacuated cavity mode frequencies are drifts of the physical lengths of the cavities and leakages and outgassing into the two cavities. To assess the influence of the former, we will simply express the evacuated cavity lengths as $L_r^{(0)}(t)$ and $L_m^{(0)}(t)$, respectively.

To assess the influence of the latter, we will first consider leakages and outgassing into an evacuated reference cavity [i.e., when the reference cavity is not completely empty but rather contains a minute amount of gas with a time-dependent nonunity index of refraction, i.e., a finite (nonzero) refractivity], which leads to a small but not insignificant drift of the index of refraction in the reference cavity, denoted $n_r^{(\mathrm{Res})}(t)$. Since the measurement cavity is being actively evacuated while the evacuated measurement cavity assessments [i.e., the $f_{(0,0)}(t_n)$ and $f_{(0,0)}(t_{n+1})$] are taken, we will assume that any leakages and outgassing into this cavity will not affect the evacuated measurement cavity assessments. This implies that the residual index of refraction in this cavity will be the same, $n_m^{(\mathrm{Res})}$, at all evacuated measurement cavity assessments, in particular when $f_{(0,0)}(t_n)$ and $f_{(0,0)}(t_{n+1})$ are assessed. This implies that the frequencies of the modes addressed in the evacuated reference and measurement cavities, $\nu_r^{(0)}(t)$ and $\nu_m^{(0)}(t)$, can be expressed as Eqs. (SM-1) and (SM-2) in Supplement 1.

The case with leakages and outgassing into the measurement cavity when it is not being evacuated, which thus constitutes a drift of Type IIb, is dealt with separately below.

G. Influence of Drifts of the Cavity Lengths, Leakages, and Outgassing into the Cavities on the Assessed Refractivity and Pressure for Various Types of Drift

1. Drifts of Type I and IIa

The assumptions leading to Eqs. (SM-1) and (SM-2) in Supplement 1 imply that it is possible to express the first- and the second-order derivatives of the mode frequencies, $\partial \nu_i^{(0)}/\partial t$ and $\partial^2 \nu_i^{(0)}/\partial t^2$, which are needed in Eqs. (20)–(26), in terms of derivatives of the evacuated cavity lengths, the residual refractive index in the reference cavity, and the leakage and outgassing rate into the measurement cavity.

As is shown by Eqs. (SM-7) and (SM-8) in Supplement 1, the derivatives for the reference cavity can be expressed in terms of $\dot{L}_r^{(0)}$, $\ddot{L}_r^{(0)}$, $\dot{n}_r^{(\mathrm{Res})}$, and $\ddot{n}_r^{(\mathrm{Res})}$, while those for the measurement cavity can be expressed in terms of $\dot{L}_m^{(0)}$ and $\ddot{L}_m^{(0)}$ (where we have used the conventional nomenclature with a single and double dot representing the first and second derivative with respect to time, respectively).

Furthermore, regarding leakages or outgassing, utilizing the fact that it is possible to express the residual refractivity in

the reference cavity, $n_r^{(\mathrm{Res})}-1$, in terms of its residual pressure as $P_r^{(\mathrm{Res})}=\varsigma_{l/o}(n_r^{(\mathrm{Res})}-1)$, where $\varsigma_{l/o}=2RT/(3A_{R,l/o})$, where, in turn, $A_{R,l/o}$ is the molar polarizability of the gas leaking (or outgassing) into the cavity, denoted l/o, makes it possible to write $\dot{n}_r^{(\mathrm{Res})}$ and $\ddot{n}_r^{(\mathrm{Res})}$ as $\dot{P}_r^{(\mathrm{Res})}/\varsigma_{l/o}$ and $\ddot{P}_r^{(\mathrm{Res})}/\varsigma_{l/o}$, respectively. This implies that the first- and the second-order derivatives of the frequency of the mode addressed in the cavity i, i.e., $\partial\nu_i^{(0)}/\partial t$ and $\partial^2\nu_i^{(0)}/\partial t^2$, can be expressed, as given by Eqs. (SM-10)–(SM-15) in Supplement 1, for the reference cavity, in terms of $\dot{L}_r^{(0)}$, $\ddot{L}_r^{(0)}$, $\dot{P}_r^{(\mathrm{Res})}$, and $\ddot{P}_r^{(\mathrm{Res})}$. By use of these expressions, and the aforementioned fact that $\delta(n-1)$ is given by $\delta(\Delta f)/\nu_m^{(0)}$, it is possible to obtain, for the various types of FPS-based refractometry methodologies addressed in this work, expressions for the errors (or uncertainties) in the assessment of refractivity from drifts of Type I and IIa, $\delta(n-1)_{\mathrm{I,IIa}}$, as given by Eqs. (SM-16)–(SM-21) in Supplement 1.

When addressing pressure of a species x, these errors (or uncertainties) provide errors (or uncertainties) in the associated pressure, $\delta P_{\mathrm{I,IIa}}$, that are given by

$$\delta P_{\mathrm{I,IIa}}=\varsigma_x\delta(n-1)_{\mathrm{I,IIa}}, \tag{27}$$

where ς_x is given by $2RT/(3A_{R,x})$.

2. Drifts of Type IIb

Leakages and outgassing into the measurement cavity while it is not being evacuated, which thus constitutes a drift of Type IIb, will not affect properties of the evacuated measurement cavity assessments. Instead, they will affect the refractivity of the gas in the measurement cavity when it is pressurized. Moreover, as long as the refractometer is assessing a pressure produced by a device under test (DUT), the gas that leaks or outgasses into the measurement cavity will replace the same amount (or pressure) of the gas that is addressed. Since the gas that leaks or outgasses into the measurement cavity can have a refractivity that is dissimilar to that of the gas addressed—the former consists of gas with a molar polarizability of $A_{R,l/o}$, while the latter is assumed to consist of a gas with a polarizability of $A_{R,x}$—despite a constant pressure, the refractivity in the cavity can, while the measurement cavity is being filled or held at a constant pressure, change an amount $\delta(n-1)_{\mathrm{IIb}}$ given by Eq. (SM-22) in Supplement 1.

Although this is a real alteration of the refractivity in the cavity, the experimentalist normally is unaware of these leakages or outgassing processes, whereby he/she will unwittingly, by the use of Eqs. (4) and (5), relate this to a molar density solely using a molar polarizability of the gas addressed, gas x, i.e., $A_{R,x}$. This will provide an error (or uncertainty) of the assessed pressure, δP_{IIb}, that is given by

$$\delta P_{\mathrm{IIb}}=\begin{cases}\left(\frac{A_{R,l/o}}{A_{R,x}}-1\right)\dot{P}_m t_{\mathrm{cmp}} & \text{for the UM methodolgies}\\ \zeta\left(\frac{A_{R,l/o}}{A_{R,x}}-1\right)\dot{P}_m t_{\mathrm{mod}} & \text{for the modulated methodolgies}\end{cases}, \tag{28}$$

where $\dot{P}_m$ is the leakage rate of gas into the measurement cavity.

H. Influence of Drifts of the Cavity Lengths, Leakages, and Outgassing into the Cavities on the Assessed Refractivity and Pressure in Various Types of Methodologies

1. UMNI Refractometry

SFPC-based refractometry: As is shown in Supplement 1 [by use of Eqs. (SM-16) and (SM-25)], which are based on Eqs. (20), (27), and (28), it is possible to express the leading term of the combined error (or uncertainty) in the assessment of pressure for conventional SFPC-based UMNI refractivity, $\delta P_{\mathrm{UMNI}}^{\mathrm{SFPC}}$, as

$$\delta P_{\mathrm{UMNI}}^{\mathrm{SFPC}}=\zeta_{\mathrm{UM}}\left[-\varsigma_x\frac{\dot{L}_m^{(0)}}{L_m^{(0)}}+\left(\frac{A_{R,l/o}}{A_{R,x}}-1\right)\dot{P}_m\right]_{t_g}t_{\mathrm{cmp}}, \tag{29}$$

where $L_m^{(0)}$ is the length of the measurement cavity, while $\dot{L}_m^{(0)}$ is its rate of change.

DFPC-based refractometry: As can be concluded from a comparison of Eqs. (20) and (21), the error (or uncertainty) in the assessment of the shift of the beat frequency from drifts of Type I or IIa for DFPC-based refractometry differs from that for SFPC-based refractometry by the fact that the former also comprises corresponding expressions (with reversed sign) for the reference cavity. Since there is no gas replacement phenomenon in the reference cavity, when the gas leaks (or outgasses) into it, the error (or uncertainty) in the assessment of pressure for conventional (UM) DFPC-based UMNI refractivity, $\delta P_{\mathrm{UMNI}}^{\mathrm{DFPC}}$, can, based on Eqs. (21), (27), and (28) [by use of Eqs. (SM-17) and (SM-25) in Supplement 1], similarly be expressed as

$$\delta P_{\mathrm{UMNI}}^{\mathrm{DFPC}}=\zeta_{\mathrm{UM}}\left\{\varsigma_x\left(\frac{\dot{L}_r^{(0)}}{L_r^{(0)}}-\frac{\dot{L}_m^{(0)}}{L_m^{(0)}}\right)+\left[-\frac{A_{R,l/o}}{A_{R,x}}\dot{P}_r^{(\mathrm{Res})}+\left(\frac{A_{R,l/o}}{A_{R,x}}-1\right)\dot{P}_m\right]\right\}_{t_g}t_{\mathrm{cmp}}, \tag{30}$$

where the $(A_{R,l/o}/A_{R,x})\dot{P}_r^{(\mathrm{Res})}$ term is not to be included in the case the reference cavity is constantly evacuated.

2. MNI Refractometry

Similarly, based on Eqs. (22), (27), and (28) [and by use of Eqs. (SM-18) and (SM-26) in Supplement 1], the error (or uncertainty) in the assessment of pressure for MNI refractometry, δP_{MNI}, can be expressed as

$$\delta P_{\mathrm{MNI}}=\zeta_M\left\{\varsigma_x\left(\frac{\dot{L}_r^{(0)}}{L_r^{(0)}}-\frac{\dot{L}_m^{(0)}}{L_m^{(0)}}\right)+\left[-\frac{A_{R,l/o}}{A_{R,x}}\dot{P}_r^{(\mathrm{Res})}+\left(\frac{A_{R,l/o}}{A_{R,x}}-1\right)\dot{P}_m\right]\right\}_{t_g}t_{\mathrm{mod}}, \tag{31}$$

where again the first term within the brackets is to be excluded in the case when the reference cavity is constantly evacuated. Since t_{mod} normally is significantly shorter than t_{cmp}, this clearly indicates that, for a given set of drifts, MNI refractometry

provides significantly less amounts of errors (or uncertainties) (often orders of magnitude less) than what conventional (DFPC-based) UMNI refractometry does.

3. UMI Refractometry

When UMI is performed, since the drifts in the lengths of the cavities are of Type I and the leakages and the outgassing into the measurement cavity are of Type IIb, the error (or uncertainty) in the assessment of pressure, δP_{UMI}, can, based on Eqs. (25), (27), and (28) [and by use of Eqs. (SM-19) and (SM-26) in Supplement 1], be written as

$$\delta P_{\mathrm{UMI}} = \begin{cases} \zeta_{\mathrm{UM}}\left[\left(\frac{A_{R,l/o}}{A_{R,x}}-1\right)\dot{P}_m\right]_{t_g} t_{\mathrm{cmp}} + \frac{\zeta_{\mathrm{UM}}(1-\zeta_{\mathrm{UM}})}{2}\left[\varsigma_x\left(\frac{\ddot{L}_r^{(0)}}{L_r^{(0)}}-\frac{\ddot{L}_m^{(0)}}{L_m^{(0)}}\right)+\frac{A_{R,l/o}}{A_{R,x}}\ddot{P}_r^{(\mathrm{Res})}\right]_{t_g} t_{\mathrm{cmp}}^2, & (a) \\ \zeta_{\mathrm{UM}}\left[\left(\frac{A_{R,l/o}}{A_{R,x}}-1\right)\dot{P}_m - \frac{A_{R,l/o}}{A_{R,x}}\dot{P}_r^{(\mathrm{Res})}\right]_{t_g} t_{\mathrm{cmp}} + \frac{\zeta_{\mathrm{UM}}(1-\zeta_{\mathrm{UM}})}{2}\varsigma_x\left(\frac{\ddot{L}_r^{(0)}}{L_r^{(0)}}-\frac{\ddot{L}_m^{(0)}}{L_m^{(0)}}\right)_{t_g} t_{\mathrm{cmp}}^2, & (b) \\ \zeta_{\mathrm{UM}}\left[\left(\frac{A_{R,l/o}}{A_{R,x}}-1\right)\dot{P}_m\right]_{t_g} t_{\mathrm{cmp}} + \frac{\zeta_{\mathrm{UM}}(1-\zeta_{\mathrm{UM}})}{2}\varsigma_x\left(\frac{\ddot{L}_r^{(0)}}{L_r^{(0)}}-\frac{\ddot{L}_m^{(0)}}{L_m^{(0)}}\right)_{t_g} t_{\mathrm{cmp}}^2, & (c) \end{cases} \tag{32}$$

for the cases when the reference cavity is: (*a*) sealed off during the entire measurement campaign (thus providing drifts of Type I), (*b*) evacuated once per gas modulation cycle (whereby the leakage and outgassing in the reference cavity are of Type IIa), and (*c*) constantly evacuated, respectively. In deriving these, we have neglected some terms in the last parts of the expressions because of their smallness; the full expressions of the cases of drifts of Type I and IIa are given by Eqs. (SM-19)–(SM-21) in Supplement 1.

4. GAMOR

For the GAMOR methodology, δP_G, can, based on Eqs. (26)–(28) [and the same expressions in Supplement 1], for the same various cases, similarly be written as

$$\delta P_G = \begin{cases} \zeta_M\left[\left(\frac{A_{R,l/o}}{A_{R,x}}-1\right)\dot{P}_m\right]_{t_g} t_{\mathrm{mod}} + \frac{\zeta_M(1-\zeta_M)}{2}\left[\varsigma_x\left(\frac{\ddot{L}_r^{(0)}}{L_r^{(0)}}-\frac{\ddot{L}_m^{(0)}}{L_m^{(0)}}\right)+\frac{A_{R,l/o}}{A_{R,x}}\ddot{P}_r^{(\mathrm{Res})}\right]_{t_g} t_{\mathrm{mod}}^2, & (a) \\ \zeta_M\left[\left(\frac{A_{R,l/o}}{A_{R,x}}-1\right)\dot{P}_m - \frac{A_{R,l/o}}{A_{R,x}}\dot{P}_r^{(\mathrm{Res})}\right]_{t_g} t_{\mathrm{mod}} + \frac{\zeta_M(1-\zeta_M)}{2}\varsigma_x\left(\frac{\ddot{L}_r^{(0)}}{L_r^{(0)}}-\frac{\ddot{L}_m^{(0)}}{L_m^{(0)}}\right)_{t_g} t_{\mathrm{mod}}^2, & (b) \\ \zeta_M\left[\left(\frac{A_{R,l/o}}{A_{R,x}}-1\right)\dot{P}_m\right]_{t_g} t_{\mathrm{mod}} + \frac{\zeta_M(1-\zeta_M)}{2}\varsigma_x\left(\frac{\ddot{L}_r^{(0)}}{L_r^{(0)}}-\frac{\ddot{L}_m^{(0)}}{L_m^{(0)}}\right)_{t_g} t_{\mathrm{mod}}^2, & (c). \end{cases} \tag{33}$$

5. Comparison of the Abilities of the Refractometry Methodologies Addressed to Reduce the Pickup of Various Types of Drifts

These expressions provide a means to compare the ability of the refractometry methodologies addressed to reduce the pickup of various types of drifts. For simplicity, we will illustrate this concept in some detail for drifts of Type I, represented by drifts the lengths of the cavities. Drifts of Type II will be shortly commented on below.

For the NI methodologies–MNI versus UMNI: It can first be observed that the introduction of modulation in NI methodologies, i.e., MNI refractometry, reduces some of the drifts that UMNI picks up. A comparison between Eqs. (31) and (30) shows that MNI picks up solely the fraction $t_{\mathrm{mod}}/t_{\mathrm{cmp}}$ of the drifts conventional DFPC-based UMNI refractometry experiences (where we for simplicity have assumed that $\zeta_{\mathrm{UM}} = \zeta_M = \zeta$). This shows that the use of modulation reduces the influence of drifts (of Type I) by an amount given by the ratio of the gas modulation time and the campaign time. For the case with t_{mod} being 100 s (which is a typical condition for GAMOR) and t_{cmp} is 24 h (which in not uncommon for systems with long thermal equilibration times), this amounts to 10^{-3}.

For the UM methodologies–UMI versus UMNI: A comparison between Eqs. (32) and (30) illustrates that also the use of interpolation reduces the amount of drift refractivity methodologies pickup in UM methodologies, *viz.*, that UMI picks up solely a fraction,

$$\frac{(1-\zeta_{\mathrm{UM}})}{2}\frac{\left(\frac{\ddot{L}_r^{(0)}}{L_r^{(0)}}-\frac{\ddot{L}_m^{(0)}}{L_m^{(0)}}\right)}{\left(\frac{\dot{L}_r^{(0)}}{L_r^{(0)}}-\frac{\dot{L}_m^{(0)}}{L_m^{(0)}}\right)} t_{\mathrm{cmp}} \tag{34}$$

of the drifts the lengths of the cavities that DFPC-based UMNI refractometry experiences. This shows though that the actual amount of improvement the interpolation brings depends on the type of drift, and, in particular, the amount of nonlinear drift, the system experiences.

GAMOR versus UMNI: It can then similarly be concluded [by a comparison between Eqs. (33) and (30)] that GAMOR, which combines modulation with interpolation, picks up solely a fraction,

$$\frac{(1-\zeta_M)}{2}\frac{\left(\frac{\ddot{L}_r^{(0)}}{L_r^{(0)}}-\frac{\ddot{L}_m^{(0)}}{L_m^{(0)}}\right)}{\left(\frac{\dot{L}_r^{(0)}}{L_r^{(0)}}-\frac{\dot{L}_m^{(0)}}{L_m^{(0)}}\right)} \frac{t_{\mathrm{mod}}^2}{t_{\mathrm{cmp}}} \tag{35}$$

of the drifts the lengths of the cavities that DFPC-based UMNI refractometry experiences.

For the interpolated methodologies–GAMOR versus UMI: A comparison between Eqs. (32) and (33) indicates, finally, that the GAMOR methodology has the ability to reduce the pickup of drift of Type I, with respect to UMI, by a factor of

$(t_{\mathrm{mod}}/t_{\mathrm{cmp}})^2$. For the same conditions as considered above, this amounts to 10^{-6}.

For the case of drifts of Type II, a similar analysis reveals that GAMOR has the ability to reduce the influence of such drifts with respect to both UMNI and UMI refractometry by a factor of $t_{\mathrm{mod}}/t_{\mathrm{cmp}}$. It is interesting to note that GAMOR has the ability to reduce the influence of drifts of Type II to the same extent it can reduce the influence of low-frequency fluctuations [37], while it can reduce drifts of Type I significantly better.

4. EXPERIMENTAL SETUP

Over the years, a variety of GAMOR instrumentation and procedures have been developed [13,14,29–31,33–36]. While the first versions utilized a simple design and were constructed to carry out proof-of-principle demonstrations [13,29,30,35], the later realizations have been gradually upgraded to improve on their performance, first regarding precision [14,30,31] and lately, accuracy [33,36]. Moreover, whereas early realizations were based upon DFPC-spacers made of Zerodur [13,29,30,35], the high resilience to drifts of GAMOR has allowed us to address cavities made of Invar [14,33,36]. This material has a number of advantages as compared to Zerodur, which makes it attractive for quantitative assessments of pressure; e.g., since it has a high thermal conductivity, it can provide high thermal homogeneity, which facilities assessment of gas temperature, and since it is a metal, it can also easily be machined [14].

Common for all GAMOR systems is that they have been based on DFPC systems with free spectral ranges (FSRs) of around 1 GHz and finesse values of 10^4. Each cavity is probed by an Er-doped fiber laser emitting light within the C34 communication channel, i.e., around 1.55 μm, that is coupled into an acoustic-optic modulator (AOM) for fast locking feedback and an electro-optic modulator (EOM) modulated at 12.5 MHz for Pound–Drever–Hall locking.

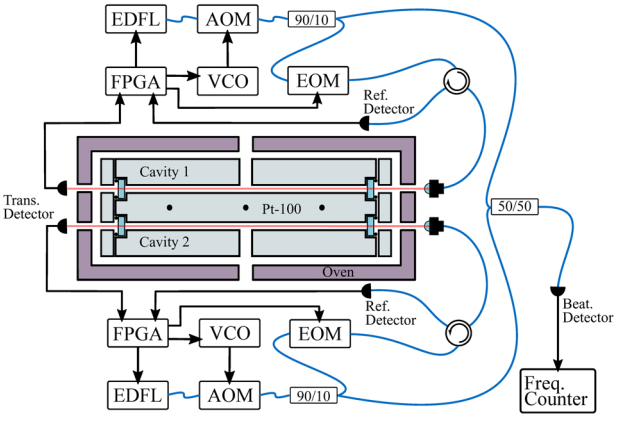

Fig. 4. Schematic illustration of the refractometry part of the experimental system. Black lines with arrows represent electrical signals, blue lines optical fibers, and red lines free-space beam paths. Each arm of the refractometer consists of an Er-doped fiber laser (EDFL), an AOM, a voltage-controlled oscillator (VCO), an EOM, a fiber splitter (90/10), and a field programmable gate array (FPGA). The beat frequency between the two arms is monitored by a detector (Beat. Detector) whose output is sent to a frequency counter. Details of the system are given in Ref. [14]. Reproduced with permission from Ref. [14].

To accommodate large shifts in cavity mode frequencies, the systems comprise an automatic relocking routine; when the wavelength-regulation feedback to a laser falls below or exceeds some preset levels, the laser makes automatically (within a fraction of a second) a controlled mode jump. To assess and regulate the temperature of the cavity spacer, in all but the earliest GAMOR instrumentation, the gas is monitored by Pt-100 sensors placed in holes drilled into the cavity spacer [14]. In addition, to assess pressure with appropriate accuracy, the most recent instrumentation has been equipped with an automated temperature regulating and assessment system in which the temperature of the spacer is assessed by the use of a thermocouple working close to zero temperature difference with respect to an automated, miniaturized, custom-made fixed-point cell based upon the well-defined melting point of gallium [33].

A schematic illustration of the Invar-based DFPC instrumentation used for the assessments in this work is shown in Fig. 4. Details of the system are given in Ref. [14].

5. RESULTS–COMPARISON OF THE ABILITY OF UMI REFRACTOMETRY, MNI REFRACTOMETRY, AND GAMOR TO MITIGATE THE INFLUENCE OF DRIFTS

A. Assessment of Data

Since a well-constructed refractometry system only shows small numbers of drifts whose presence and magnitude can be elusive and difficult to quantify, to quantitatively assess to which degree various methodologies are capable of mitigating drifts, it is advisory to address a system in which there are significant and quantifiable numbers of drifts. To validate the predictions derived in Section 3, experimental investigations have therefore, in this work, been made on a refractometry system that is deliberately affected by a substantial amount of drift, *viz.*, one not in thermal equilibrium. This does not imply that the abilities of the various methodologies addressed to mitigate the influence of drift only appear (or are of importance) in systems with significant amounts of drift; on the contrary, they take place also in well-stabilized systems with less amounts of drifts.

To clearly illustrate and quantitatively assess the ability of these methodologies to reduce the influence of drifts (in particular to assess their dependencies on the length of the gas modulation cycle, while clearly separating the influence of temperature-induced drift of the cavity length from the temperature dependence that originates from the conversion of pressure from molar density by the use of an equation of state), measurements were taken from the Invar-based refractometry system described above with the measurement cavity being constantly evacuated while the temperature of the cavity spacer was increased from room temperature (23°C) to the melting temperature of Ga (which is at 29.76°C). As a result of this, the length of both cavities increased monotonically during this process. Since the changes in length of the two cavities were not identical (the heating process affected the two cavities in a slightly dissimilar manner), the beat frequency between the two laser fields drifted over time. Figure 5 shows a period of 56 h of this 91.5 h long heating procedure, for simplicity henceforth referred to as the measurement campaign. The data show

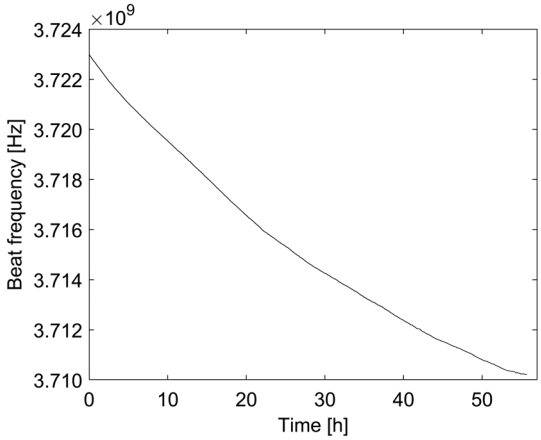

Fig. 5. Temperature-induced drift in the Invar-based DFPC refractometry system expressed as the assessed beat frequency as a function of time during 56 h of a 91.5 h long heating process during which the temperature of the system was increased from room temperature (23°C) to the melting point of Ga (29.76°C), here referred to as the measurement campaign.

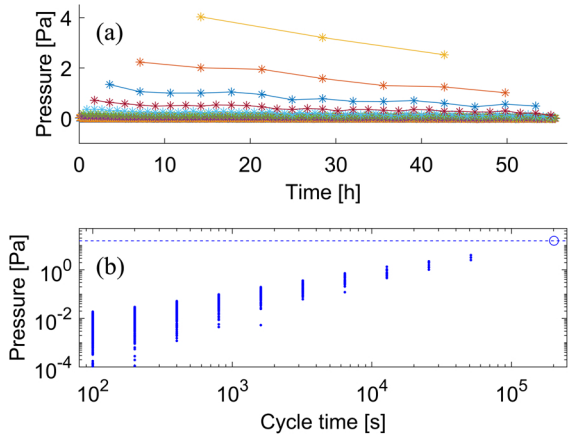

Fig. 6. Pressure evaluated from the empty cavity measurements displayed in Fig. 5 evaluated by the NI methodologies. (a) Pressure evaluated by the MNI refractometry methodology, i.e., δP_{MNI}, for 10 different gas modulation cycle lengths (from the lowermost to the uppermost: 100, 200, 400, 800, 1600, 3200, 6400, 12,800, 25,600, and 51,200 s); (b) same entity as a function of the length of the gas modulation cycle. For each gas modulation cycle length, each individual data point represents the pressure assessed by a single gas modulation cycle. The open circle in (b) at 201,600 s represents the assessed pressure evaluated by the UMNI methodology (with the assessment of the measurement cavity frequency performed after half of the campaign time, i.e., with $\zeta_{\mathrm{UM}} = 0.5$ and $t_{\mathrm{cmp}} = 201,600$ s), i.e., $\delta P^{\mathrm{DFPC}}_{\mathrm{UMNI}}$. For comparison with the MNI assessments, the level of this assessment is illustrated by the dashed line. Note the logarithmic scale of (b).

that this temperature-induced change gave rise to a drift of the lengths of the cavities that, over this period of time, decreased the detected beat frequency, 13 MHz.

Since a shift in beat frequency of $\delta(\Delta f)$ mainly corresponds to a shift in refractivity, $\delta(n-1)$, of $\delta(\Delta f)/\nu_m^{(0)}$ and a shift in pressure, δP, of $\varsigma_x \delta(\Delta f)/\nu_m^{(0)}$, where $\nu_m^{(0)}$ for the light used takes a value of 1.93×10^{14} Hz and $\varsigma_x/\nu_m^{(0)}$ for nitrogen takes, under room temperature conditions, a value of 1.86 Pa/MHz [36], this implies that, over the period of time addressed, this drift corresponds to an apparent shift in refractivity of 6.7×10^{-8}, which represents an apparent change in pressure of 24 Pa.

To assess the ability of the various methodologies addressed above to reduce the influence of drifts (to assess the influence of both interpolation and the length of the gas modulation cycle on the pickup of the drifts), the data shown in Fig. 5 were evaluated by appropriate data evaluation procedures of the four methodologies addressed above, first the NI methodologies (UMNI and MNI refractometry) followed by the interpolated ones (UMI refractometry and GAMOR), where the modulated methodologies were evaluated for 10 different gas modulation cycle lengths, ranging by factors of 2 from 100 to 51,200 s.

B. Ability of the NI Methodologies to Mitigate the Influence of Drifts

Figure 6 shows the result from an evaluation of the data displayed in Fig. 5 by use of NI refractometry, i.e., by the UMNI and MNI methodologies. Panel (a) shows, by the individual markers, the assessed pressure as a function of time for MNI refractometry (thus δP_{MNI}) for the set of gas modulation cycle lengths (from the lowermost set to the uppermost: 100, 200, 400, 800, 1600, 3200, 6400, 12,800, 25,600, and 51,200 s). Panel (b) displays, by the small-dot markers, the same data as a function of the length of the gas modulation cycle, t_{mod}. The open circle at 201,600 s represents the assessed pressure when evaluated by the UMNI methodology, i.e., $\delta P^{\mathrm{DFPC}}_{\mathrm{UMNI}}$, (which thus solely produces a single data point, with the assessment of the measurement cavity frequency carried out after half of the campaign time, i.e., with $\zeta_{\mathrm{UM}} = 0.5$). Since the assessments are made by an evacuated measurement cavity, all the assessments displayed represent deviations from the true value (which is 0 Pa). Hence, they all represent the error from the drift of the data each methodology picks up under various conditions.

First, panel (b) shows that the pressure assessed by the UMNI methodology provided a value of 15.6 Pa. It also shows that the pressures assessed by the MNI methodology, which range from 4 Pa into the sub-millipascal region, are consistently below that of the UMNI methodology.

Second, panel (a) indicates that the pressure assessed by the MNI methodology decreases (predominantly) monotonically with time, in qualitative agreement with the general behavior of the assessed beat frequency in Fig. 5, which, in turn, originates from the fact that the system is successively approaching stable temperature conditions. This implies that in Fig. 6(b), in which every group of MNI markers represents a given cycle length and each individual marker in each group corresponds to an individual gas modulation cycle assessment, the uppermost assessments result in general from the first part of the measurement campaign (in which the drift is largest) while the lowermost ones originate from its last part. These data do not only show that for each gas modulation length, there is a significant spread in assessed pressure, they also show that the assessed pressure decreases with decreasing gas modulation cycle length. The values range, for the longest gas modulation cycle (51,200 s), from 4.0 to 2.5 Pa, and, for the shortest (100 s), from 19 mPa

and downwards (with some assessments outside the scale of the plot, i.e., in the sub-0.1 mPa region).

These MNI data confirm qualitatively the alleged statement that the length of the time separation between the evacuated and the filled measurement cavity assessments has a significant impact on the error (or uncertainty) of the assessments. It thus supports the assumption that a modulation procedure, with its short gas modulation cycle length, efficiently can mitigate the influence of drifts on assessments of refractivity, molar density, and pressure by refractometry.

It is interesting to note that the MNI assessments also quantitatively are in good agreement with the predictions by the dominating sources of errors (or uncertainties) in MNI refractometry that to leading order are given by Eq. (22). Since it is possible to estimate, from Fig. 5, that the difference in linear drift of the two cavities, i.e., $(\partial \nu_r^{(0)}/\partial t)_{t_g} - (\partial \nu_m^{(0)}/\partial t)_{t_g}$, ranges from 120 to 20 Hz/s over the time period addressed, and since ζ takes a value of 0.5, Eq. (22) indicates that the expected shift in beat frequency should, for the case with the longest gas modulation cycle (51,200 s), range from 3 to 0.5 MHz (via values of 2.2 and 1.3 MHz at the time instances for the first and the last data points in the data set, taken after 14 and 42 h, respectively), which correspond to shifts in pressure ranging from 6 to 1 Pa (via 4.1 and 2.4 Pa at the same two time instances). This is in good agreement with the data shown in Fig. 6, which, for the same gas modulation cycle length and the same two time instances, provide 4.0 and 2.5 Pa, respectively.

The same expression predicts that, for the shortest gas modulation cycle (100 s), the assessed shift in beat frequency should range from 6 to 1 kHz, which corresponds to shifts in pressure ranging from 10 to 2 mPa. Although the assessed pressure for each modulation cycle ranges from 19 mPa and downwards, the values for the first part of the data set gravitates around 12 mPa (19 mPa is a single outlier), this is likewise in good agreement with the findings shown in Fig. 6. This confirms the validity of Eq. (22) for MNI refractometry.

C. Ability of the Interpolated Methodologies to Mitigate the Influence of Drifts

A similar analysis for the interpolated methodologies displays an even more potent ability to mitigate the influence of drifts. Figure 7 shows, by its two panels, a corresponding evaluation of the same set of data (the evacuated measurement cavity assessments displayed in Fig. 5) by the interpolated methodologies (GAMOR and UMI). Panel (a) shows the assessed pressure as a function of time for the GAMOR methodology for the 10 different gas modulation cycle lengths (100 to 51,200 s), while panel (b) displays the same entity as a function of gas modulation cycle length. The open circle at 201,600 s represents here the assessed pressure when evaluated by the UMI methodology, providing a single value of δP_{UMI} of 3.6 Pa. Note the difference in scale between the panels (a) in Figs. 6 and 7.

First, a comparison of the UMI data point in Fig. 7 with the UMNI data in Fig. 6, which are 3.6 and 15.6 Pa, respectively, provides a first verification of the assumption that interpolation (in this case, between the first and the last parts of the measurement campaign) can serve as a means to reduce the pickup of drifts.

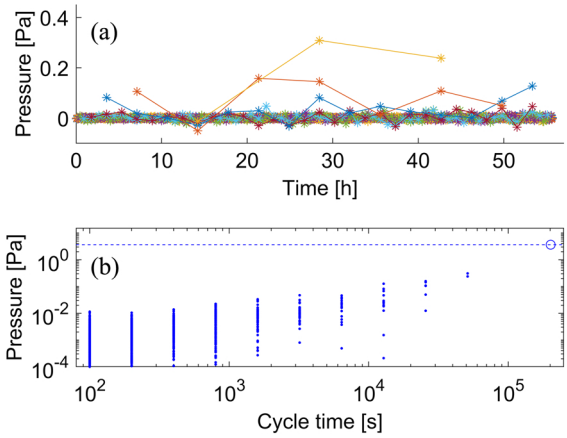

Fig. 7. Pressure evaluated from the empty cavity measurements displayed in Fig. 5 evaluated by the interpolated methodologies. (a) Pressure evaluated by the GAMOR methodology, i.e., δP_G, for the same 10 gas modulation cycle lengths as in Fig. 6, i.e., 100–51,200 s; (b) same entity as a function of the length of the gas modulation cycle. Each individual data point represents an individual pressure assessment for the given gas modulation cycle length. The open circle in (b) represents the assessed pressure when evaluated by the UMI methodology with the assessment of the measurement cavity frequency after half of the campaign time (i.e., that with $\zeta_{\mathrm{UM}} = 0.5$ and $t_{\mathrm{cmp}} = 201,600$ s), i.e., δP_{UMI}. For comparison with the GAMOR assessments, the level of this assessment is illustrated by the dashed line. Note the logarithmic scale of (b).

Second, a comparison of the panels (b) in Figs. 6 and 7 indicates that the maximum assessed pressures by GAMOR for each cycle length, which for the longest gas modulation cycle (51,200 s) is 0.3 Pa and for the shortest (100 s) 11 mPa, are consistently lower than those assessed by use of the MNI methodology (which ranged from 4 Pa downwards). This confirms the alleged statement that, irrespective of whether modulation is used or not, interpolation can mitigate the influence of drifts on assessments of refractivity, molar density, and pressure by FP-based refractometry.

Third, panel (b) reveals that the GAMOR-assessed pressures are consistently lower than those assessed by use of the UMI methodology. This confirms the alleged statement that, even when interpolation is used, the modulation procedure can additionally mitigate the influence of drifts on assessments of refractivity, molar density, and pressure by refractometry.

The GAMOR data are also in good agreement with the estimates based on the leading order contribution to the errors (or uncertainties), given by Eq. (18). It can, from Fig. 5, be concluded that the difference in second-order derivatives of the beat frequency, i.e., $(\partial^2 \nu_r^{(0)}/\partial t^2)_{t_g} - (\partial^2 \nu_m^{(0)}/\partial t^2)_{t_g}$, for the longest cycle lengths (51,200 s), takes values that range from 5×10^{-4} Hz/s^2 and downwards. Since $\zeta(1-\zeta)/2 = 1/8$, this implies that Eq. (18) predicts a contribution to the beat frequency for this gas modulation cycle length of 0.16 MHz, which corresponds to a pressure of 0.3 Pa, while for a cycle length of 100 s, it corresponds to 0.6 Hz, which represents a pressure in the sub-0.1 mPa range. While the estimated data for the longest cycle length (0.3 Pa) agree very well with the ones evaluated by the GAMOR methodology [uppermost curve in Fig. 7(a)], the estimates for the shortest modulation cycle length are far below

the assessed ones [given by the leftmost group of data points in Fig. 7(b)]. In this case, the errors in the assessments originate predominantly from other types of processes, e.g., noise and fluctuations, not addressed in this work. The data taken at the longer cycle lengths verify well though the predictions given by the Eq. (18) above.

D. Comparison between the Abilities of UMI and MNI Refractometry to Mitigate the Influence of Drifts

The data above also provide a possibility to compare the relative advantages of interpolation over gas modulation regarding the ability to mitigate drifts. Figure 7(b) shows that the UMI methodology provides a pressure value of 3.6 Pa, while Fig. 6(b) shows that the MNI methodology picks up pressure assessments that range from 4 Pa and downwards, with those corresponding to 100 s cycle lengths consistently being below 19 mPa. This indicates that MNI has the ability to outperform UMI when it comes to reduction of the influence of the drift of the data in Fig. 5.

E. Comparison between the Abilities of the Modulated Methodologies to Mitigate the Influence of Drifts

The data also provide a possibility to compare the benefit of interpolation for the modulated methodologies (MNI and GAMOR) regarding the ability to mitigate drifts. Since the true value of an assessment of refractivity (and thereby pressure) in an evacuated measurement cavity is 0 Pa, it is possible to estimate the uncertainty of the assessments for a particular gas modulation cycle length of the modulated methodologies as the root mean square of all pressures assessed over the entire measurement campaign at that particular cycle length, δP_{RMS}. Performing such an analysis of the data given above provides, for the MNI refractometry methodology, the uncertainties shown by the black markers in the upper curve in Fig. 8. These data show that the uncertainty in the assessment decreases significantly with decreased length of the gas modulation cycle, from 3.3 Pa (for a gas modulation cycle length of 51,200 s) to 7 mPa (for a length of 100 s). The lower set of data represents the corresponding cases for the GAMOR methodology. These data again indicate that the uncertainties in the assessments are consistently lower than for the MNI methodology and that they decrease with decreased length of the gas modulation cycle lengths, in this case, from 0.2 Pa to 2 mPa for same set of gas modulation cycle lengths.

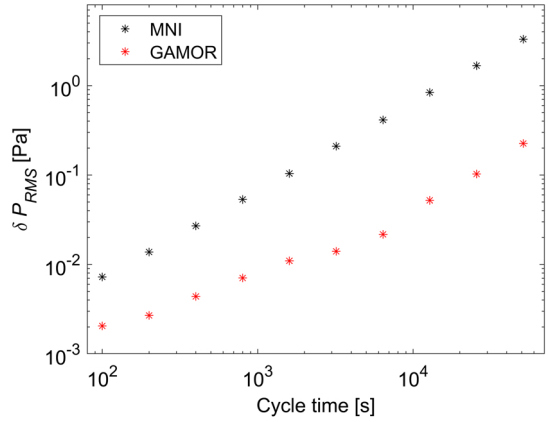

Fig. 8. Error (or uncertainty) in the assessment of pressure, δP_{RMS}, for a given modulation cycle length, defined as the root mean square of the assessed pressures, as a function of the length of the modulation cycle evaluated by the use of MNI refractometry and the GAMOR methodology, given by the uppermost and lowermost data sets, respectively.

This illustrated the advantage of GAMOR over the MNI methodology when the data contain drifts.

6. SUMMARY AND CONCLUSIONS

It has previously been both prophesized and shown experimentally that the GAMOR methodology has the ability to reduce the influence of noise, fluctuations, and drifts on refractometry assessments [13,14,29–32,35]. In an early realization, it was demonstrated that the methodology was capable of reducing drifts from a DFPC-based refractometry system with no active temperature control by up to 3 orders of magnitude, from the pascal to the millipascal range [30]. More recently, a GAMOR system has demonstrated, when assessing pressure at 4303 Pa, a minimum Allan deviation of 0.34 mPa, which corresponds to a relative deviation of 0.08 ppm [14]. This extraordinary ability has been attributed to a measurement procedure that is based upon two cornerstones: (i) one being that the refractivity of the gas in the measurement cavity is assessed by the use of a rapid gas modulation procedure that allows for a repetitive referencing of the filled measurement cavity beat frequency assessments to evacuated cavity assessments, while (ii) the other is that the evacuated measurement cavity beat frequency is estimated based on an interpolation between two assessed evacuated measurement cavity beat frequency measurements.

It has been alleged that both these features contribute to the extraordinary ability of the methodology to reduce the number of fluctuations and drifts the methodology picks up, which, in turn, improves on its precision [32]. It was recently shown that cornerstone (*i*) provides the GAMOR methodology with an ability to significantly reduce the influence of periodic disturbances, referred to as fluctuations, in the system [32]. However, hitherto, the fundamental cause for the ability of the GAMOR methodology to reduce the influence of slow (monotonic) disturbances, denoted drifts, has not yet been elucidated. This work has therefore scrutinized this issue.

Using a Taylor-series-based model of drifts of the frequencies of the cavity modes, expressions are derived that illustrate how drifts affect the assessed shift in beat frequency and thereby refractivity and pressure in various types of FPC-based refractometer systems. A comparison between the expressions for the influence of drifts on the conventional FPC-based UMNI methodologies [i.e., either Eqs. (20) and (21) or Eqs. (29) and (30)] reveals that while conventional SFPC-based UMNI refractivity is limited by *the drift of the frequency of the mode addressed in the measurement cavity* (and thereby primarily the *linear drifts* in the length of the measurement cavity and its residual pressure) during the time between the empty and filled cavity assessments, i.e., t_{cmp}, conventional DFPC-based UMNI refractivity is affected only by the *difference* in drifts of the frequencies of the modes addressed in the two cavities (and thereby primarily the *difference* in the linear drift rates of

the length of the two cavities) during the same time interval. On the other hand, the latter is additionally affected by leakages and outgassing in the reference cavity. This illustrates the well-known fact that if a DFPC spacer can be made so that the differential drift is significantly smaller than the common drift, i.e., if $|(\partial \nu_r^{(0)}/\partial t)_{t_g} - (\partial \nu_m^{(0)}/\partial t)_{t_g}| < |(\partial \nu_m^{(0)}/\partial t)_{t_g}|$, and the leakages and outgassing in the reference cavity can be held low, DFPC-based refractometry will be considerably less affected by drifts than SFPC-based refractometry.

Although, at first glance, it might seem that MNI refractometry does not bring in any significant advantage as compared to conventional DFPC-based UMNI refractometry regarding the influence of drifts [since their responses, given either by Eqs. (21) and (22) or Eqs. (30) and (31), have the same parametric dependence]; in reality, it does so. There are two reasons for this. The first is that the repetitive assessments in modulated refractometry provide a time separation between the gas filling and emptying processes (then referred to as the gas modulation cycle time) that is significantly shorter than in conventional DFPC-based UMNI refractometry; it is, for the modulated methodologies, given by a fraction ζ_M of the gas modulation cycle time, i.e., $\zeta_M t_{\mathrm{mod}}$, while for conventional UMNI refractometry methodologies, it is given by the time separation between the evacuated and filled measurement cavity assessments, i.e., $\zeta_{\mathrm{UM}} t_{\mathrm{cmp}}$. By this, any given drift will affect the measurement significantly less in the modulated methodologies than in the UM ones: for the case with t_{mod} being 10^2 s and t_{cmp} 10^5 s, by up to 3 orders of magnitude less.

The second is that the repetitive assessment allows for a large number of assessments during a limited time; still for the case when t_{mod} is 10^3 times smaller than t_{cmp}, the modulated methodologies allow for 10^3 gas modulation cycles for each gas filling-and-emptying process in the conventional UMNI refractometry methodologies. This opens up for the possibility of an averaging process that will allow for both a reduction of white noise (in the case considered, by a factor of 30) [31] and a significant reduction of the influence of fluctuations (between a factor of unity and 10^3, depending on the Fourier frequency of the fluctuation) [32].

As was alluded to above, cornerstone (*ii*) provides GAMOR with additional advantages regarding the influence of campaign-persistent drifts, i.e., drifts of Type I. Equation (26) [as well as Eq. (33)] shows, first of all, that the GAMOR methodology does not have any dependence on the linear part of such drifts; it is only affected by their nonlinear parts. This originates from the fact that cornerstone (*i*) converts the linear parts of the drifts to small amount of errors (or uncertainties) [given by Eq. (22) as well as Eq. (31)] that cornerstone (*ii*) thereafter, by its interpolation procedure, effectively eliminates. The linear parts of the drifts of Type I will therefore not contribute to the error (or uncertainty) in the GAMOR signal. This thus verifies the alleged property that GAMOR is immune to the dominating linear parts of campaign-persistent drifts [14,30,31].

Equations (26) and (33) additionally reveal that for drifts of Type I, GAMOR is solely affected by the *difference in the nonlinear parts of the drifts* of the two cavities (i.e., the difference in the nonlinear parts of the changes of the lengths of two cavities, and, for the case with a sealed-off reference cavity, also the difference in the nonlinear part of the leakages and outgassing into the reference cavity). In addition, a comparison first between Eqs. (20)–(26), and then Eqs. (29)–(33), shows that while the influence of drifts decreases linearly with the time between the assessments of the evacuated and filled measurement cavity assessments for the conventional UMNI methodologies as well as MNI refractometry, for the interpolated methodologies (i.e., the UMI methodology and GAMOR), it decreases, for drifts of Type I, quadratically with the same time period. Moreover, the maximum value of $\zeta(1-\zeta)/2$ is 1/8, which additionally reduces the influence of drifts of Type I.

For the other types of drift (i.e., for cycle-limited drifts from leakages and outgassing of Type IIa or IIb), the UMI methodology and GAMOR are affected by drifts as the MNI methodology, i.e., by the difference in their linear drifts over the gas modulation cycle time.

An important difference between the UM and the modulated methodologies (either UMNI and MNI refractometry, or UNI refractometry and GAMOR) is that the modulated ones are functions of the length of the gas modulation time, t_{mod}, while the others depend on the length of the measurement campaign, t_{cmp}. Since it is not uncommon that $t_{\mathrm{mod}}/t_{\mathrm{cmp}}$ is in the order of 10^{-3}, the modulated methodologies can outperform the UM ones by up to 3 orders of magnitude for drifts of Type II, and up to 6 orders of magnitude for drifts of Type I.

Experiments show that a refractometer that is exposed to deliberately induced temperature drifts giving rise to a change in beat frequency, that, when evaluated according to conventional DFPC-based UMNI refractometry, corresponds to an apparent change in pressure of 24 Pa will, when analyzed by use of UM interpolation (i.e., the UMI methodology) provide pressure with a smaller error (solely 3.6 Pa). When, on the other hand, the same data are evaluated as if they would have modulated (i.e., by the MNI methodology), it will give rise to apparent pressures ranging solely between 3.3 Pa and 17 mPa (given as RMS values, for cycle lengths of 51,200 and 100 s, respectively). When the GAMOR methodology is used, the corresponding numbers are 0.2 Pa and 2 mPa, respectively. It is also shown that these numbers agree with the predicted mitigations given by the leading order terms of the expression for the evaluation of pressure.

This shows that the modulated methodologies indeed have the ability to reduce the influence of drifts, and more so the shorter the gas modulation cycle length, and additionally more when interpolation is used for the assessment of the empty measurement beat frequency (i.e., when GAMOR is performed), in the present case (when GAMOR is used with a gas modulation cycle length of 100 s) by more than 4 orders of magnitude (from 24 Pa to 2 mPa). Naturally, for the cases with less drifting refractometry systems, the relative advantage of the modulated methodologies might not be as large as this, since they can only reduce the uncertainties to levels corresponding to other sources of disturbances, but they will, nevertheless, in all cases mitigate the influence of drifts.

For the case when the refractometry system is exposed to significant amounts of drifts, and in particular when high pressures are addressed, it is possible that a GAMOR-based system is limited by residual nonlinear drift components. In such cases, it is possible to extend the interpolation procedure to be based on more than two evacuated measurement cavity assessment

data points (e.g., four) and make use of a nonlinear fit for the estimated evacuated measurement cavity beat frequency. By this, the influence of not only the linear but also the quadratic component of the drift can be eliminated.

All this indicates that the modulated refractometry methodologies in general, and GAMOR in particular, have significantly better ability to mitigate the influence of drifts on the assessment of refractivity, molar density, and pressure than the conventional UMNI refractometry methodologies. It also implies that they can be used with excellent performance under a variety of conditions, including not fully stabilized ones.

Funding. European Metrology Programme for Innovation and Research (18SIB04); Vetenskapsrådet (621-2015-04374, 621-2019-04159); Umeå Universitet (The Industrial Doctoral School (IDS) programme); VINNOVA (2018-04570, 2019-05029); Kempe Foundation (1823, U12).

Disclosures. The authors declare no conflicts of interest.

Data Availability. Data underlying the results presented in this paper are not publicly available at this time but may be obtained from the authors upon reasonable request.

Supplemental document. See Supplement 1 for supporting content.

REFERENCES AND NOTES

1. P. F. Egan, J. A. Stone, J. H. Hendricks, J. E. Ricker, G. E. Scace, and G. F. Strouse, "Performance of a dual Fabry-Perot cavity refractometer," Opt. Lett. **40**, 3945–3948 (2015).
2. M. Andersson, L. Eliasson, and L. R. Pendrill, "Compressible Fabry-Perot refractometer," Appl. Opt. **26**, 4835–4840 (1987).
3. L. R. Pendrill, "Density of moist air monitored by laser refractometry," Metrologia **25**, 87–93 (1988).
4. M. L. Eickhoff and J. L. Hall, "Real-time precision refractometry: new approaches," Appl. Opt. **36**, 1223–1234 (1997).
5. N. Khelifa, H. Fang, J. Xu, P. Juncar, and M. Himbert, "Refractometer for tracking changes in the refractive index of air near 780 nm," Appl. Opt. **37**, 156–161 (1998).
6. H. Fang and P. Juncar, "A new simple compact refractometer applied to measurements of air density fluctuations," Rev. Sci. Instrum. **70**, 3160–3166 (1999).
7. L. R. Pendrill, "Refractometry and gas density," Metrologia **41**, S40–S51 (2004).
8. E. Hedlund and L. R. Pendrill, "Improved determination of the gas flow rate for UHV and leak metrology with laser refractometry," Meas. Sci. Technol. **17**, 2767–2772 (2006).
9. E. Hedlund and L. R. Pendrill, "Addendum to 'Improved determination of the gas flow rate for UHV and leak metrology with laser refractometry (vol 17, pg 2767, 2006),'" Meas. Sci. Technol. **18**, 3661–3663 (2007).
10. P. Egan and J. A. Stone, "Absolute refractometry of dry gas to +/- 3 parts in 10^9," Appl. Opt. **50**, 3076–3086 (2011).
11. I. Silander, M. Zelan, O. Axner, F. Arrhen, L. Pendrill, and A. Foltynowicz, "Optical measurement of the gas number density in a Fabry-Perot cavity," Meas. Sci. Technol. **24**, 105207 (2013).
12. D. Mari, M. Bergoglio, M. Pisani, and M. Zucco, "Dynamic vacuum measurement by an optical interferometric technique," Meas. Sci. Technol. **25**, 125303 (2014).
13. I. Silander, T. Hausmaninger, M. Zelan, and O. Axner, "Fast switching dual Fabry-Perot cavity optical refractometry—methodologies for accurate assessment of gas density," arXiv:1704.01186v2 (2017).
14. I. Silander, C. Forssén, J. Zakrisson, M. Zelan, and O. Axner, "Invar-based refractometer for pressure assessments," Opt. Lett. **45**, 2652–2656 (2020).
15. M. Zelan, I. Silander, C. Forssén, J. Zakrisson, and M. Zelan, "Recent advances in Fabry-Perot-based refractometry utilizing gas modulation for assessment of pressure," Acta IMEKO **9**, 299–304 (2020).
16. I. Silander, C. Forssén, J. Zakrisson, M. Zelan, and O. Axner, "Optical realization of the Pascal—characterization of two gas modulated refractometers," J. Vac. Sci. Technol. B **39**, 044201 (2021).
17. K. Jousten, J. Hendricks, D. Barker, K. Douglas, S. Eckel, P. Egan, J. Fedchak, J. Flugge, C. Gaiser, D. Olson, J. Ricker, T. Rubin, W. Sabuga, J. Scherschligt, R. Schodel, U. Sterr, J. Stone, and G. Strouse, "Perspectives for a new realization of the pascal by optical methods," Metrologia **54**, S146–S161 (2017).
18. A common way to assess such a shift is to mix the frequency of the laser light down to a radio frequency (RF) by the use of another laser (a reference laser). This can practically be achieved by merging the two laser fields onto a photodiode. By this, the beat frequency between the two can be measured directly from the photodiode response by the use of a frequency counter. This implies that the shift in the frequency of the cavity mode addressed when gas is let into the cavity is converted to a shift in a measured beat frequency.
19. F. Riehle, P. Gill, F. Arias, and L. Robertsson, "The CIPM list of recommended frequency standard values: guidelines and procedures," Metrologia **55**, 188–200 (2018).
20. R. W. Fox, B. R. Washburn, N. R. Newbury, and L. Hollberg, "Wavelength references for interferometry in air," Appl. Opt. **44**, 7793–7801 (2005).
21. G. Z. Xiao, A. Adnet, Z. Y. Zhang, F. G. Sun, and C. P. Grover, "Monitoring changes in the refractive index of gases by means of a fiber optic Fabry-Perot interferometer sensor," Sens. Actuators A Phys. **118**, 177–182 (2005).
22. L. P. Yan, B. Y. Chen, E. Z. Zhang, S. H. Zhang, and Y. Yang, "Precision measurement of refractive index of air based on laser synthetic wavelength interferometry with Edlen equation estimation," Rev. Sci. Instrum. **86**, 085111 (2015).
23. J. H. Hendricks, G. F. Strouse, J. E. Ricker, D. A. Olson, G. E. Scace, J. A. Stone, and P. F. Egan, and NIST, "Photonic article, process for making and using same," U.S. patent US20,160,018,280 A (March 20, 2015).
24. P. F. Egan, J. A. Stone, J. E. Ricker, and J. H. Hendricks, "Comparison measurements of low-pressure between a laser refractometer and ultrasonic manometer," Rev. Sci. Instrum. **87**, 053113 (2016).
25. T. Rubin and Y. Yang, "Simulation of pressure induced length change of an optical cavity used for optical pressure standard," J. Phys. Conf. Ser. **1065**, 162003 (2018).
26. H. Fang, A. Picard, and P. Juncar, "A heterodyne refractometer for air index of refraction and air density measurements," Rev. Sci. Instrum. **73**, 1934–1938 (2002).
27. A. Picard and H. Fang, "Three methods of determining the density of moist air during mass comparisons," Metrologia **39**, 31–40 (2002).
28. J. A. Stone and A. Stejskal, "Using helium as a standard of refractive index: correcting errors in a gas refractometer," Metrologia **41**, 189–197 (2004).
29. M. Zelan, I. Silander, T. Hausmaninger, and O. Axner, "Fast switching dual Fabry-Perot-cavity-based optical refractometry for assessment of gas refractivity and density—estimates of its precision, accuracy, and temperature dependence," arXiv:1704.01185v2 (2017).
30. I. Silander, T. Hausmaninger, M. Zelan, and O. Axner, "Gas modulation refractometry for high-precision assessment of pressure under non-temperature-stabilized conditions," J. Vac. Sci. Technol. A **36**, 03E105 (2018).
31. I. Silander, T. Hausmaninger, C. Forssén, M. Zelan, and O. Axner, "Gas equilibration gas modulation refractometry for assessment of pressure with sub-ppm precision," J. Vac. Sci. Technol. B **37**, 042901 (2019).
32. O. Axner, I. Silander, C. Forssén, J. Zakrisson, and M. Zelan, "Ability of gas modulation to reduce the pickup of fluctuations in refractometry," J. Opt. Soc. Am. B **37**, 1956–1965 (2020).
33. I. Silander, C. Forssén, J. Zakrisson, M. Zelan, and O. Axner, "An Invar-based Fabry-Perot cavity refractometer with a gallium fixed-point cell for assessment of pressure," Acta IMEKO **9**, 293–298 (2020).
34. C. Forssén, I. Silander, D. Szabo, G. Jönsson, M. Bjerling, T. Hausmaninger, O. Axner, and M. Zelan, "Transportable refractometer for assessment of pressure in the kPa range with ppm level precision," Acta IMEKO **9**, 287–292 (2020).

35. O. Axner, I. Silander, T. Hausmaninger, and M. Zelan, "Drift-free Fabry-Perot-cavity-based optical refractometry—accurate expressions for assessments of refractivity and gas density," arXiv:1704.01187v2 (2017).
36. J. Zakrisson, I. Silander, C. Forssén, M. Zelan, and O. Axner, "Procedure for robust assessment of cavity deformation in Fabry–Pérot based refractometers," J. Vac. Sci. Technol. B **38**, 054202 (2020).
37. Axner *et al.* [32] considered disturbances in refractometry systems that can be described in terms of a set of Fourier components with Fourier frequencies, f_D, that constitute an integer number of inverse measurement campaign times, t_{cmp}. That work showed to which extent fluctuations can be eliminated by GAMOR. It was demonstrated that it can, on the average, reduce the influence of fluctuations with Fourier frequencies, f_D, between $1/(\pi t_{\mathrm{cmp}})$ and $1/(\pi t_{\mathrm{mod}})$ by an amount of $(\pi f_D t_{\mathrm{mod}})^{-1}$ and those with a Fourier frequency around $1/(\pi t_{\mathrm{cmp}})$, by $t_{\mathrm{cmp}}/t_{\mathrm{mod}}$ [32].
38. Disturbances that take place at longer time scales than fluctuations [so long that their Fourier frequencies are lower than the inverse of π times the measurement campaign time, i.e., $< 1/(\pi t_{\mathrm{cmp}})$] are here considered as, and denoted, drifts.
39. All methodologies modeled have in common that they fill and evacuate one cavity, referred to as the measurement cavity, while the other cavity is considered to be a reference cavity, held under constant conditions.
40. Neglecting any possible influence of a finite but minute penetration depth of light into the mirrors, since this plays no role in the assessment of the ability of GAMOR to reduce or eliminate the influence of drifts.
41. Although GAMOR can be performed by several different modes of operation [29,30], we will in this work restrict ourselves to analysis of its original realization, in which the amount of gas in one of the cavities is regularly modulated, while that in the other one is held constant [29]. This has most in common with the modes of operation of (conventional) UM DFPC-based refractivity and allows therefore for a direct and straightforward comparison of the two methodologies.
42. A. D. Buckingham and C. Graham, "Density dependence of refractivity of gases," Proc. R. Soc. London A **337**, 275–291 (1974).
43. M. Puchalski, K. Piszczatowski, J. Komasa, B. Jeziorski, and K. Szalewicz, "Theoretical determination of the polarizability dispersion and the refractive index of helium," Phys. Rev. A **93**, 032515 (2016).
44. If large densities (or high pressure) of gas are to be assessed, additional higher-order terms need to be added in Eqs. (4) and (5).
45. K. Jousten, "Temperature relaxation of argon and helium after injection into a vacuum vessel," Vacuum **45**, 1205–1208 (1994).
46. J. Ricker, K. O. Douglass, S. Syssoev, J. Stone, S. Avdiaj, and J. H. Hendricks, "Transient heating in fixed length optical cavities for use as temperature and pressure standards," Metrologia **58**, 035003 (2021).
47. For the case when the drifts are of Type IIb [so they affect the (amount or type) of gas in the measurement cavity] $\Delta f(t_g, t_g)$ no longer constitutes a drift-free assessment]. The influence of this type of drift is addressed separately in Section 3.G.2.
48. This implies that their Taylor series expansions of the evacuated cavity mode frequencies, given by Eq. (7), are appropriately valid also outside a single gas filling-and-emptying period or gas modulation cycle, in particular at the time of the second evacuated cavity measurement assessment at t_{n+1}, as illustrated by the uppermost blue solid curve in Fig. 3.
49. A short gas modulation cycle time also allows for, within a given campaign time, a large number of repeated measurements, which, in turn, allows for both a reduction of the influence of fluctuations [31] and an averaging of a large number of individual assessments that will reduce disturbances (noise) of white type [30].
50. If needed, corrected for any possible residual gas pressure in the evacuated measurement cavity according to the procedure given elsewhere [30]. In addition, to reduce the influence of high-frequency fluctuations or spurious disturbances, Δf is often assessed as an average over a number of beat frequency assessments (e.g., over 10 s) around t_g [35].
51. T. Rubin, I. Silander, M. Bernien, J. Zakrisson, M. F. Hao, C. Forssén, A. Kussicke, P. Asbahr, M. Zelan, and O. Axner are preparing a manuscript to be called "Thermodynamic effects in a gas modulated Invar-based dual Fabry-Pérot cavity refractometer."